Alma Mater Studiorum - Università di Bologna

SCUOLA DI SCIENZE

Dipartimento di Chimica Industriale "Toso Montanari"

Corso di Laurea Magistrale in

Chimica Industriale

Classe LM-71 - Scienze e Tecnologie della Chimica Industriale

Tesi di Laurea sperimentale

Dithienopyrrole-based materials: development of new polymeric derivatives

CANDIDATO

Silvia Quattrosoldi

RELATORE

Prof. Elisabetta Salatelli

CORRELATORE

Prof. Guy Koeckelberghs

Pieter Leysen

Anno Accademico 2016-2017

ABSTRACT

The possibility to control molar mass and termination of the growing chain is fundamental to create well-defined, reproducible materials. For this reason, in order to apply polydithienopyrrole (PDTP) as organic conjugated polymer, the possibility of controlled polymerization needs to be verified. Another aspect that is still not completely explored is bound to the optical activity of the PDTP, which bearing appropriate substituents may adopt a helical conformation. The configuration of the helix, built up from achiral co-monomers, can be established in an enantiopure way by using only a small percentage of the chiral monomer co-polymerized with achiral co-monomer. The effect, called "sergeants and soldiers effect", is expressed by the nonlinear increase of the chiral response vs the ratio of the chiral co-monomer used for the polymerization. To date, this effect is still not completely explored for PDTP.

In this framework the project will investigate, firstly, the possibility to obtain a controlled polymerization of PDTP. Then, monomers with different side chains and organometallic functions will be screened for a CTCP-type polymerization. Also a Lewis-acid based cationic polymerization will be performed. Moreover the chemical derivatization of dithienopyrrole DTP is explored: the research is going to concern also block copolymers, built up by DTP and monomers of different nature.

The research will be extended also to the investigation of optically active derivates of PDTP, using a chiral monomer for the synthesis. The possibility to develop a supramolecular distribution of the polymeric chains, together with the "sergeant and soldiers effect" will be checked investigating a series of polymers with increasing amounts of chiral monomer.

SUMMARY

CHAPTER 1: CONJUGATED POLYMERS

1.1 Characteristics of conjugated polymers

In the last years, conjugated polymers have attracted increased attention due to their ability to conduct electrical current upon appropriate doping. These materials could be a real alternative in the development of electric devices, with all the benefits connected with organic semiconductors. Despite the overall good performance of inorganic semiconductors, their organic counterparts are adopted more and more as replacement. Conjugated polymers boast several attractive properties: the most important, is the solubility in common organic solvents. This property allows materials to be easily cast.[1] The benefits are not only connected to processability, but also to the intrinsic nature of polymers. Lightness, flexibility and resistance against corrosion are other properties that contribute to assert conjugated polymers in the industrial field. Moreover the specific properties, the attractive aspect regards also the possibility to easily derivate monomer/polymer with simple structural alteration. It is indeed easy to manipulate optic and electronic properties of material and control how it performs in semiconducting devices.[2]

The ability of organic conjugated material to conduct lies within the π – conjugated system, *i.e* a series of sp^2-hybridized atoms with overlapping p-orbitals. The orbitals are oriented perpendicular to the polymer backbone allowing for an electronic interaction between the double bonds, that permit to create a π molecular orbital extended through the chain. Increasing the number of conjugated bonds, the number of π - molecular orbitals and π* - molecular orbitals increase (Figure 1.1.1).

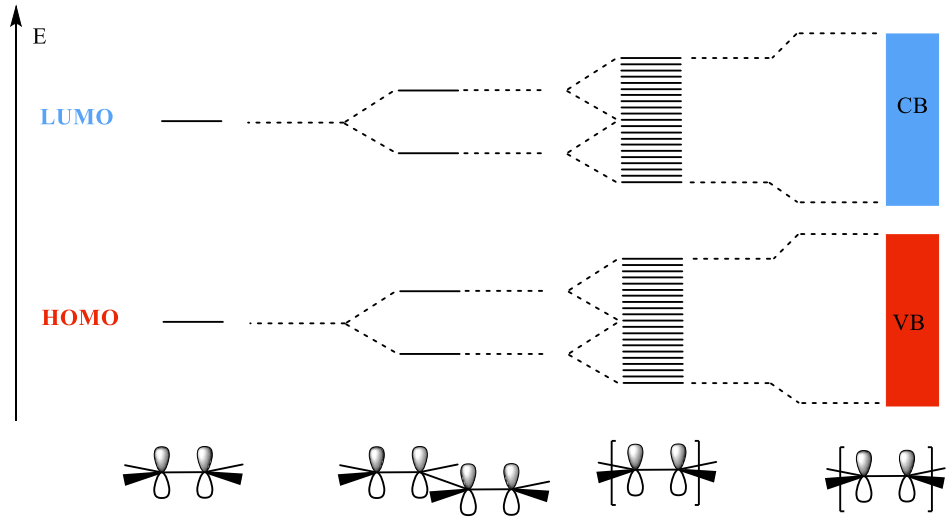

Figure 1.1.1: Formation of energy bands in conjugated polymers

In this fashion, the energy of the highest occupied molecular orbital (HOMO) increases, while the energy of the lowest unoccupied molecular orbital (LUMO) decreases, thus reducing the energetic gap (E_g) between the bands.[3]

The first example of a conjugated polymer was polyacetylene, whose features were discovered in 1977 by MacDiarmid, Heeger, and Shirakawa [4,5,6,7]. They were awarded the Nobel Prize for their discovers in 2000. Despite the original interest in polyacetylene, conjugated polymers derived from heterocycles have received the most attention. This increased attention was the result of several factors, such as better chemical and physical stability compared to polyacetylene, but mostly for the better performance of the derivate devices. Indeed, the number of electrons in the conjugated system increase and the E_g decreases (Figure 1.1.2).

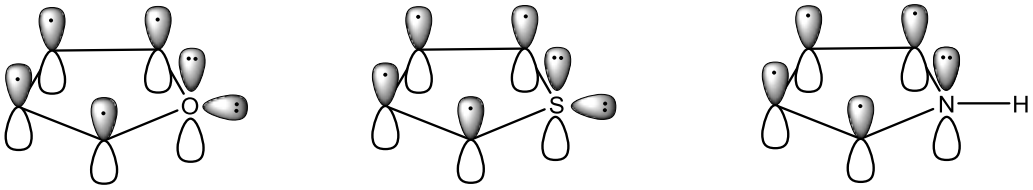

Figure 1.1.2: Orbital structures of heterocyclic molecules

To expand on polythiophene, chemists designed and synthesized new polyheterocycles with different architectures to tune the electronic/optical properties. One approach involves

increasing the planarity of the conjugated backbone by minimizing steric interactions, as these tend to cause backbone twisting and affect the conjugation. A strategy to avoid twisting is to design monomers with rigid structures, for example a bridging unit between two adjacent cycles.[8] In that way, the rotation around the inter-nuclear bond is impossible. Band gap tuning of conjugated polymers is not only limited to the planarity of the system. Another synthetic strategy is based on the inductive or resonance effects by the introduction of electron-donating and electron-withdrawing functional groups along the polymer backbone.[9] The nature of the functional groups affects the MOs: the incorporation of electron-donating substituents such as alkyls, alkoxyls, amines, or electron rich chalcogens increases the ionization potential and raises the HOMO level of aromatic molecules; while using electron-withdrawing substituents (fluorides, imines, nitriles, nitro groups..) increases the electron affinity and results in lower LUMO levels.[10] Normally, the two effects are combined together in one monomer comprised of electron withdrawing groups and electron donating groups. The presence of these, in particular in the side chains at the bridging unit, allows the functionalized molecule to remain symmetrical, thus reducing possible problems with regio regularity.[11]

1.2 Characteristics of chiral conjugated polymers

Another way to tune the behavior of conjugated polymers is to induce chiral organization. The macromolecular chains may arrange in two different ways: the polymer adopts a chiral conformation as helicoidal structure (Figure 1.2.1, a). This is well represented by poly(3,6-carbazole)s, gallic acid substituted poly(dithienopyrrole)s, oxazoline-functionalized poly(thiophene)s and poly- (3,6-polyphenanthrene)s. [12,13,14,15] Otherwise the chains, adopting a planar and achiral conformation, may organize in a macromolecular arrangement (Figure 1.2.1, b).

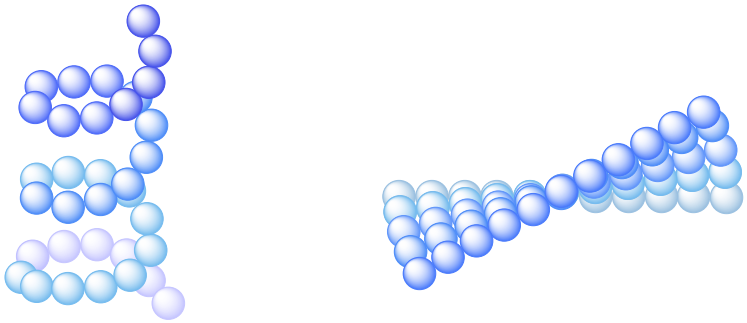

Figure 1.2.1: a) Helicoidal conformation of one single chain, b) Achiral polymeric chains stacked in a chiral way

In most cases conjugated polymers tend to aggregate; indeed they use to stay in a planar conformation and π-interaction facilitates the stacking between chains, forming a chiral structure. This organization is accompanied by red shift in the absorption spectrum.[16]

The ways to introduce a chiral center are different, the easiest method is to functionalize the side chain of the molecules. Alternative methodology is to perform a polymerization between a chiral monomer and an achiral derivate. Some groups have reported the introduction of a chiral alignment using chiral moieties such as chiral binaphthol and cyclohexanediamine. The chirality can also be achieved by noncovalent interactions between the polymer and chiral solvents or chiral side chains or chiral moieties etc.[16]

Considering helical polymers prepared from a chiral monomer, it is known that the specific chirality of the monomer promotes mostly one of the two helical possible states. This happens also if only a percent of a chiral derivate is polymerized in presence of achiral monomer. This phenomenon is called “sergeants and soldiers” principle, where the chiral monomers act as “sergeants” that force the “soldiers”, the achiral monomer, to adopt one helical sense. The experimental proof of this behavior is expressed by the nonlinear increase of the chiral response to monomer ratio. Indeed, presence of small amount of chiral monomer leads to a large enantiomeric excess.

The first chiral conjugated polymer, a polyacetylene derivate, was prepared by Ciardelli and coworkers in 1973.[17] The interest around this new material continued to grow and a lot of research groups started to investigate the possibility to insert chirality in every well-known conductive polymeric system. The first synthesis of a heterocycle- based conjugated polymer

(Cp) was reported in 1988 by Lamaire and coworkers, who synthetized a chiral polythiophene by electropolymerization.[18] In that way, it was possible to match the good electronic performance of Cp's with the optical properties introduced by the asymmetric centers. As a consequence, a new generation of optoelectronic materials was born.

The studies have been focused not only on homopolymeric chiral derivatives, but also on copolymers. Indeed the use two of different monomers in different ratios and the possibility to introduce chirality, further expands the application field. A lot of investigations were preformed by Green, who observed that poly(isocyanate) obtained by chiral and achiral monomers randomly bounded, resulted in an helical structure.[19] Regarding block-co-polymers, Van den Bergh and coworkers focused their research on block copolymers composed by HT- poly(3-alkylthiophene) (P3AT) and a HT- poly(3-alkoxythiophene) (P3AOT) block. The result obtained showed that the first block can pose limitations on the aggregation behavior of the second block, resulting in macro- and supramolecular properties which are not found in the corresponding homopolymers.[20]

For chiral compounds, an unequal absorption of left and right circularly polarized light can exist. The emergent linear polarized light becomes elliptically polarized; this unequal absorption of left and right polarized light is referred as "circular dichroism". This is expressed by the difference of the molar extinction coefficient of the absorbed left-handed circularly polarized light (ε_L) and right-handed circularly polarized light (ε_D) (Eq 1).

$$\Delta\varepsilon = \varepsilon_L - \varepsilon_D \tag{1}$$

$$\theta = 32.90 * \Delta\varepsilon * l * c \tag{2}$$

Where ε is the molar extinction coefficient, θ is the angle of deviation of the light, l is pathlength, c is the concentration.

Circular dichroism is one of the most sensitive and powerful techniques for the measurement of the chiroptical proprieties of chiral molecules, and thus also for chiral polymers.

The chiroptical behavior combined with the conductivity typical of conjugated polymers has found a wide field of applications such as asymmetric electrosynthesis, polarization sensitive electro-optical devices etc. But, compared to the knowledge that the scientific community has about conjugated polymers, the information concerning to chiral conjugated polymers is still limited.[21]

1.3 Controlled polymerization

Controlled polymerizations have always attracted attention by the scientific community. The ability to control growth and termination of polymer chains is a useful tool to build an advanced material with well defined characteristics. Controlled polymerization was studied by Michael Szwarc and coworkers.[22] They determined that in chain growth condition, in absence of termination and transfer, the number of propagating polymer chains must remain constant and the rate of polymerization for each growing chain must be equal. In this situation, the degree of polymerization and hence the molar mass of the polymer can be predicted by the monomer to initiator ratio. Moreover, it is also possible to control the end groups of the polymeric chain.[23,24]

1.3.1 Catalyst transfer condensative polymerization (CTCP)

One example of controlled polymerization technique is the catalyst transfer condensative polymerization. The mechanism involves a cross coupling reaction with transition metals. The polymerization consists of:

- oxidative addition (OA)
- transmetallation (TM)
- reductive elimination (RE)

In 2004, Yokozawa and McCullough independently discovered that a particular polymerization, *i.e*. the synthesis of poly(3-alkylthiophene) (P3HT) with a Ni(dppp)Cl_2 catalyst, proceeds in a controlled chain growth fashion.[25,26,27] The mechanism, explained later, was made possible by complexation of the catalyst to the π system of the growing polymer. The catalyst remains complexed to the polymer after reductive elimination and is then transferred to terminal C- halogen bond where the oxidative addition takes place. The fundamental part of this kind of polymerization is the interaction between polymer and

catalyst, that always remains complexed to the polymer chain. Excessive interaction as well as scarce interaction of this complex, can hamper the polymerization.[28]

Kumada Method

One of the most investigated technique is the Kumada catalyst transfer condensative polymerization (KCTCP), which uses the Kumada-coupling, a coupling between halide and a Grignard function.[29] This synthesis requires particular attention because the organometallic compound is very sensitive to moisture: the magnesium derivate is generated in situ, starting from a precursor monomer.

During the initiation, two different transmetallations occur, where two monomers react with the catalyst, exchanging with two halogens (Scheme 1.3.1).[30]

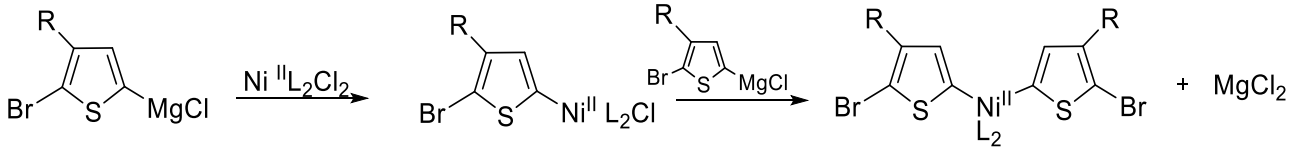

Scheme 1.3.1: Transmetallation

Subsequent reductive elimination (Scheme 1.3.2) gives rise to a tail to tail dimer. The catalyst complexes with the dimer and the following oxidative addition occurs intermoleculary with one of the two Br atoms.

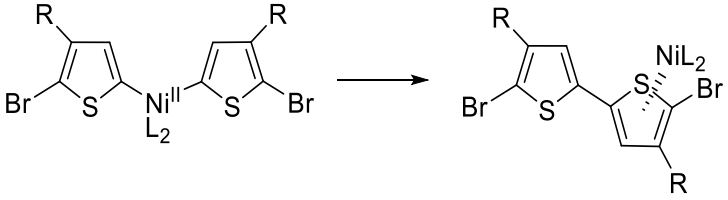

Scheme 1.3.2: Reductive elimination

Upon completion of the initial transmetallation, reductive elimination, oxidative addition, the same cycle is repeated during the propagation. Between reductive elimination and oxidative

addition, the catalyst remains associated to the polymer backbone. In this way, transfer and termination reactions are suppressed.

The most used catalysts for the KCTCP are Ni and Pd-based; the former metal permits a higher degree of control over the polymerization, therefore is more studied than Pd. Nickel catalyst promotes a tail to head polymerization; moreover, it was proved that the sterical demand plays an important role in the regioregularity of the finale product. [31,32]

However, there are many examples of controlled polymerization conducted also in presence of $Pd(PPh_3)_4$ as catalyst.[29] The main problem with Pd is its weaker association to the backbone; the use electron donating ligands was attempted in order to modify the behavior of Pd.

The KCTCP regioregularity can also be influenced by LiCl. This salt breaks up the aggregated Grignard reagents and forms ate-complexes: this increases the propagation rate and facilitates the formation of head to head couplings.[31]

1.3.2 Acid catalyzed cationic polymerization

Another way to obtain a controlled polymerization is via living cationic polymerization. Since the discovery in 1980 by Higashimura and Kennedy, this polymerization was a great breakthrough because previous cationic polymerizations were poorly controlled.[33,34]

In order to start a cationic polymerization, an initiation step is necessary. Here the active specie, normally an unstable cation, is formed. This species adds to the monomer, forming a stable cation (tertiary or secondary) that can propagate. In order to produce an active center an acid initiator reacts with a basic monomer (nucleophilic). Inorganic Lewis acids are one of the most popular polymeric initiators.

The mechanism, reported in Scheme 1.3.3, shows a cationic polymerization via $SnCl_4$.[35]

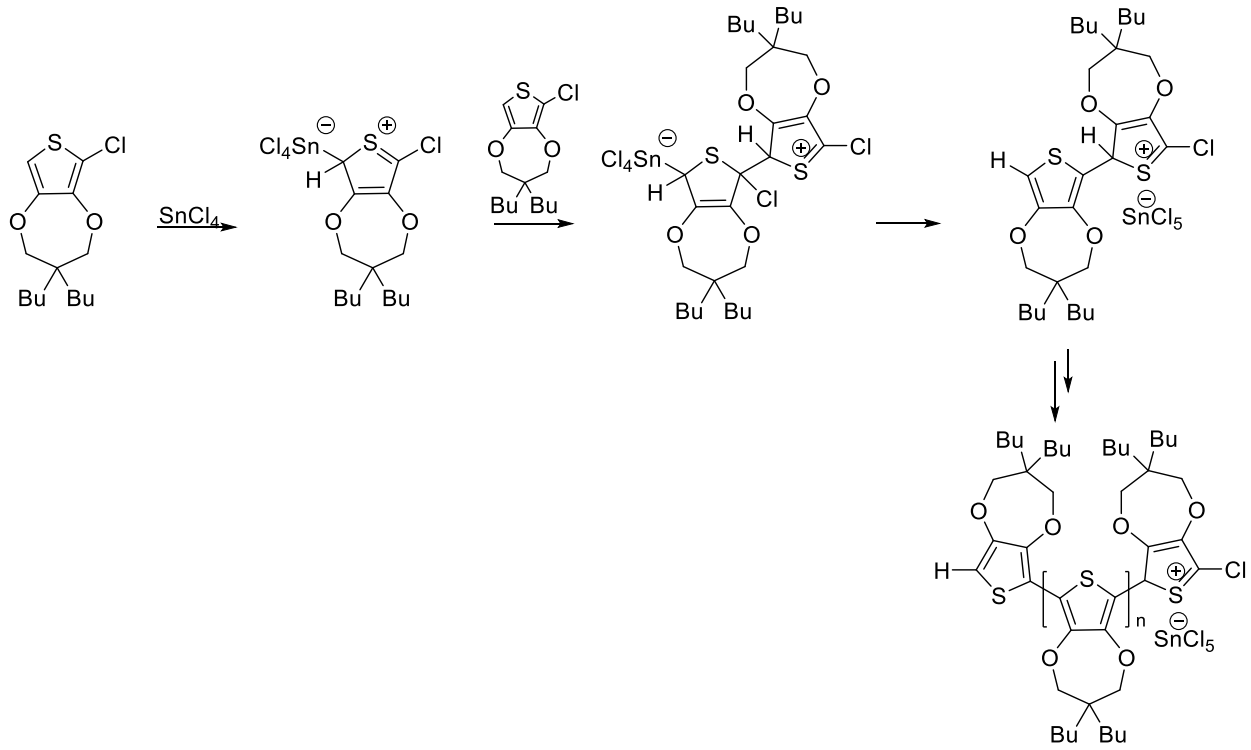

Scheme 1.3.3: Proposed mechanism for cationic polymerization via $SnCl_4$

The carbocation formed reacts with monomer, increasing the length of the polymer chain (Scheme 1.3.3). Termination does not occur between two propagating chains but between two different ions, forming a new neutral compound. If during polymerization a strong acid is formed, it could react with free Lewis acid to create a very strong Brønsted acid. Under these conditions, the growing polymer is protonated, reducing the degree of propagating species, and HCl complexation of the Lewis acid lowers its effectiveness as a catalyst.[35] In addition, polar groups interacting with the Lewis acid, may retard the polymerization. By choosing the right Lewis acid, it is possible to improve the polymerization. According to Olah, $SnCl_4$ and $FeCl_3$, compared with $AlCl_3$, have strong affinity for halogen atoms.[36] The $SnCl_4$-induced polymerization rate for O- or N-containing monomers was shown to be 103 –105 times larger than the rates with the conventional Et_xAlCl_{3x} (x 1.25 or 1.5) initiating systems. The difference in polymerization behavior between $EtAlCl_2$ and $SnCl_4$ can be explained. The first aspect that is necessary to consider, is the different chemical nature: $SnCl_4$ is considered a soft acid, whereas Al-based Lewis acids are considered hard. Because of its softness, $SnCl_4$ interacts weakly with polar functional groups and attacks the relatively soft halogens atom more readily

than its aluminum counterpart. Moreover, the counterion is also crucial to achieve high reactivity of the system: $SnCl_4$ produces a stable hexacoordinated anion coordinated to the monomer. On the other hand, the counterion from $EtAlCl_2$ is tetrahedral and unstable.

1.4 Dithienopyrrole

Dithieno[3,2-*b*:2',3'-*d*]pyrrole (DTP) (Figure 1.4.1) contains all the previously mentioned strategies to optimize the behavior of the conductive polymer. Indeed, the monomer consists of heteroatom bridge and can be properly functionalized.

Since initial studies by Zanirato and coworkers in 1983, DTP has received increased attention: due to its properties and several sites for functionalization, DTP derivatives have found applications in several fields. [10,11,37] The most studied DTP derivatives are *N*-functionalized with an alkyl or aryl side chain. Commonly, these monomers are defined as first generation, due to recent development of second generation DTPs, characterized by electron-withdrawing acyl side chains. [11]

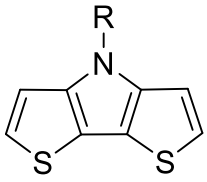

Figure 1.4.1: Dithieno[3,2-*b*:2',3'-*d*]pyrrole

1.4.1 Synthesis of monomer

First generation

As mentioned, Zanirato and coworkers reported the synthesis of unfunctionalized DTP for the first time in the 1983.[37] Then, Zotti developed a method to generate *N*-functionalized DTPs in yields of ~70% to increase solubility.[38] Nevertheless, the number of synthetic steps and the overall low yield limited the application as conductive polymers. Therefore, during the last

years several research groups have worked around synthesis to obtain a new optimized method.[38,39,40,41]

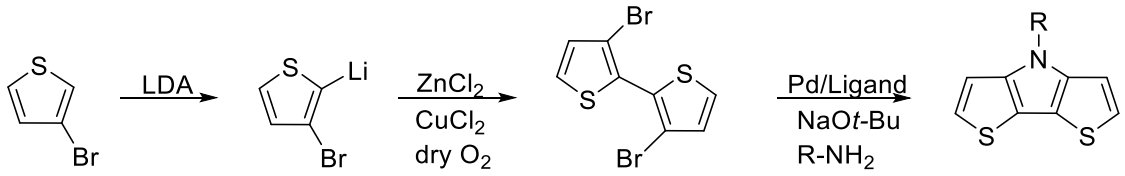

Scheme 1.4.1: Optimized synthesis of 2,2'-dibromothiophene

As shown in Scheme 1.4.1, lithium diisopropylamide (LDA) is used to generate the lithiated intermediate by selective deprotonation. The additional use of $ZnCl_2$ and $CuCl_2$ with dry O_2 enhances the efficiency of the oxidative coupling step to give increased yield: the molecule obtained is stable and easy to handle. The last step is a Pd-catalyzed coupling: using a double Buchwald–Hartwig reaction (Scheme 1.4.2), two new C-N bonds are obtained. During the starting step, a precatalyst forms a Pd(0)−ligand complex that undergoes oxidative addition with the aryl electrophile. The nucleophilic amine is complexed to the metal and deprotonated by the base. The catalytic cycle is ended by reductive elimination, which forms the final arylated amine product while regenerating the active catalyst. In order to complete the catalytic cycle, the nature of the ligand is fundamental and is also a tool to modify the final product.[40]

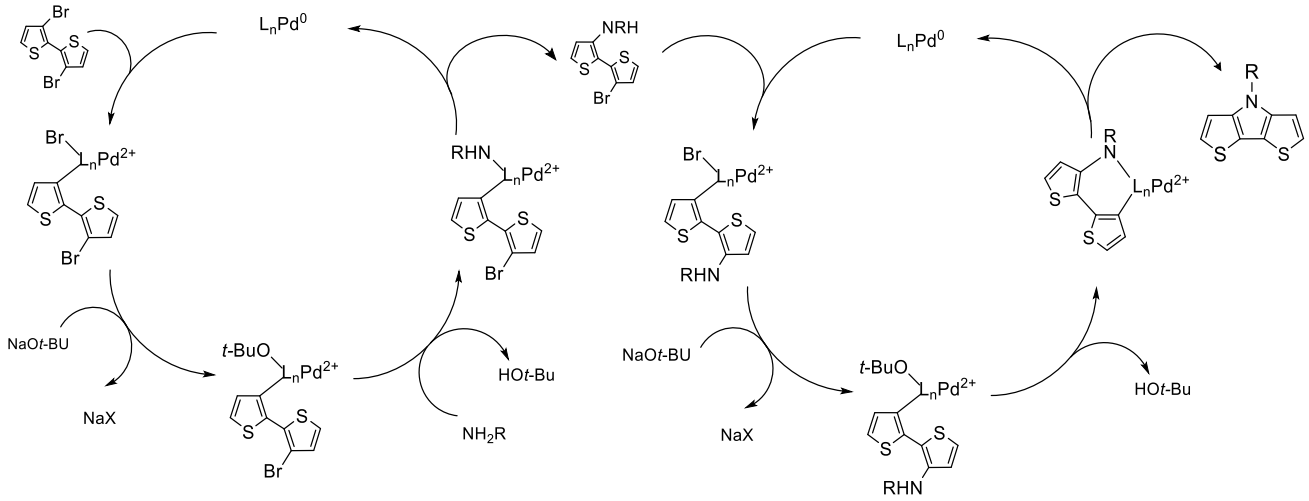

Scheme 1.4.2: Buchwald - Hartwig cycle

Second generation

In the last few years, a new class of DTP has been synthetized. The second generation monomers exhibit a stabilized HOMO level thanks to presence of acyl group bound to the N atom. The first attempt to synthetize this new derivate monomer via copper catalyzed amination of 3,3'-dibromo-2,2'–bithiophene, had poor yield (40%).[39] It is believed that the resulting *N*-acylDTP inhibits the catalyst, thus limiting further production of the desired product. Attempts to apply the Pd-catalyzed method that successfully generated first generation DTPs for the production of second generation monomers, resulted in insoluble product.

Not a lot has been reported on the second generation PDTPs; Evenson and coworkers published the electropolymerization of an *N*-acylDTP derivate, obtaining the corresponding homopolymer.[39]

1.4.2 Synthesis of polymer

First generation

The first synthesis of the polymeric material was reported by Zotti and coworkers in 1992, who polymerized a series of DTP derivates via electropolymerization.[38] Until 2000, no new studies were reported around this polymer. Then, Rasmussen published a new method based on the oxidative polymerization of *N*-functionalized DPT, via $FeCl_3$.[39,42,43] The main problem of this procedure was the molecular amount of oxidized material that hampered the formation of polymer with high molar mass. The method was modified and good results were obtained with $CuCl_2$ and $RuCl_3$. In 2007, different methodologies not based on the oxidative process, but focused on coupling reaction were proposed. In particular, the polymerization via Stille coupling became quite popular thanks to the good yield (50/60 %) (Scheme 1.4.3). The benefits of the organostannanes based reaction are the stability of the reagent to air and moisture. Moreover, the process is highly compatible with different functional groups, eliminating extra reactions for protection and deprotection. But, in order to obtain a good yield, the catalysts have to be optimized as well as the reaction conditions. Moreover, Stille coupling reactions are quite sensible to the thermal stability of the substrate and the stereo/regiospecificity of the system.[41,44]

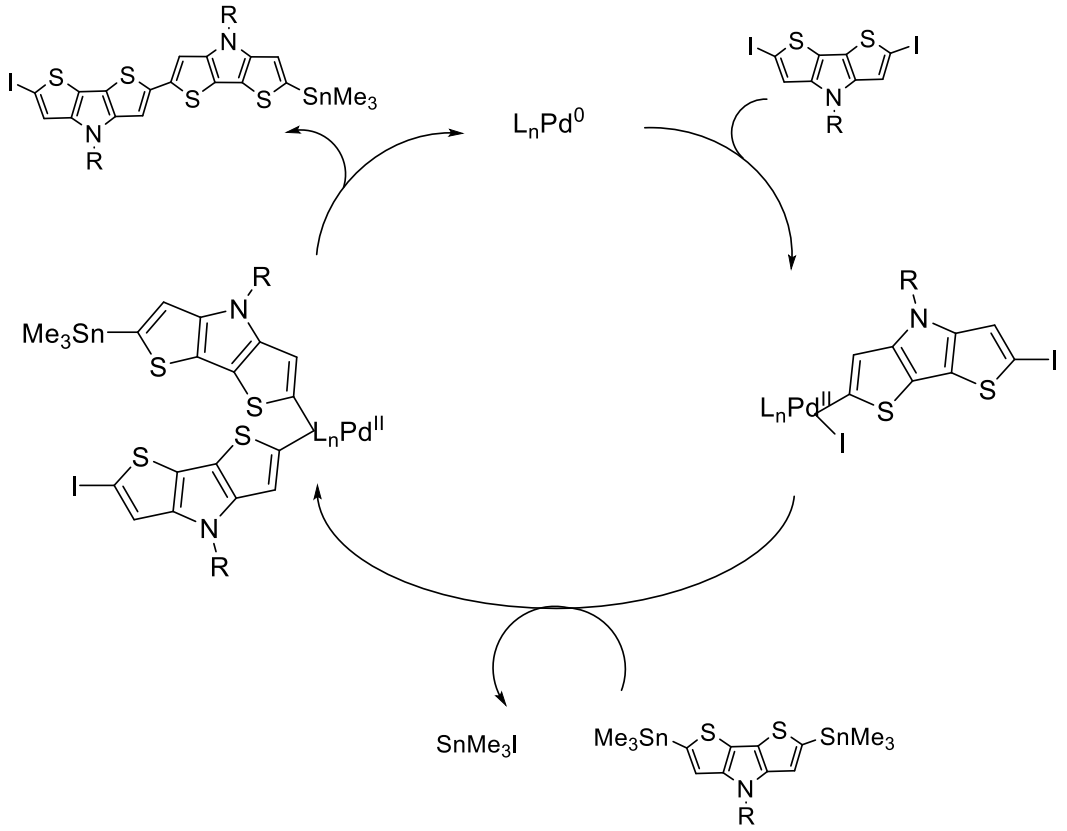

Scheme 1.4.3: Stille coupling

A different approach was followed by the Yamamoto-type polymerization (Scheme 1.4.4). The reaction is a coupling using bis(1,5-cicloottadiene) nichel $Ni(COD)_2$ as reagent in the presence of 2,2′-bipyridine (Bpy).[13,41]

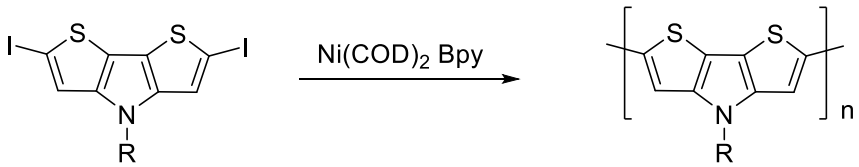

Scheme 1.4.4: Yamamoto polymerization

The yield obtained with this methodology was too low to produce real development. Further studies about the yield showed that is dependent on the amount of insoluble material after polymerization. The Stille polymerization, where the polymers were completely soluble, showed the highest yield. These conditions seem to promote the formation of high molecular mass polymeric material. GPC analysis reveals that the polymers prepared by a Stille reaction had a significantly higher molecular mass than the polymers prepared by oxidative or Yamamoto-type polymerization. These two methodologies showed multimodal weight distribution and as a result high polydispersity. Despite Stille-couplings showed a lower polydispersity, the polymerization conditions known to now are far from controlled. Controlled polymerizations are not yet described, but are a concrete possibility, similarly to P3HT, that is well prepared in a controlled polymerization using KCTCP.[27,45]

The studies around PDTP developed also in the direction of copolymers; the first example was reported in 1997.[46] (Figure 1.4.1 a)

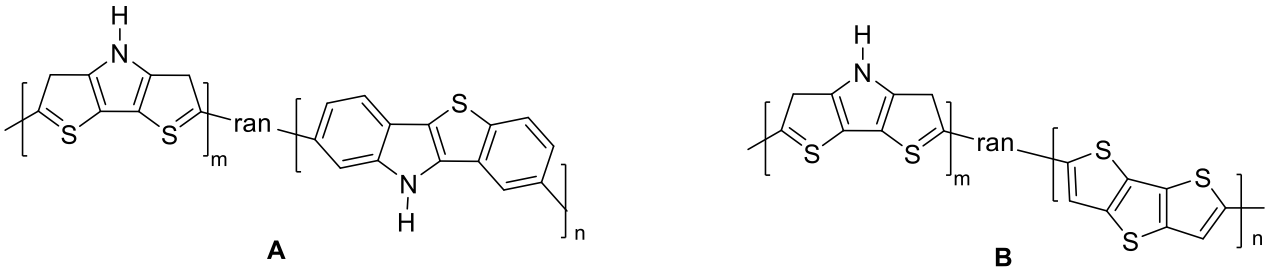

Figure 1.4.1: first examples of random copolymers

Absence of conductivity and electrochromic properties in films with less than 70% of DTP was observed for the copolymer (A). Moreover, it was proved that the monomer was responsible for the proprieties of the final polymeric material. Another example of a random copolymer (Figure 1.4.1 B) shows good conductivity and electrochromic properties at any monomers ratio used.[47] The copolymer investigation was also conducted by Qin and coworkers, who in 2008 published the first examples of soluble and processable copolymeric materials of DTP. The polymerization was performed by a Suzuki polycondensation between 2,6-diboroester DTP with various dibromoarene systems in order to synthetize the alternating DTP-arylene copolymers (Scheme 1.4.5).[48]

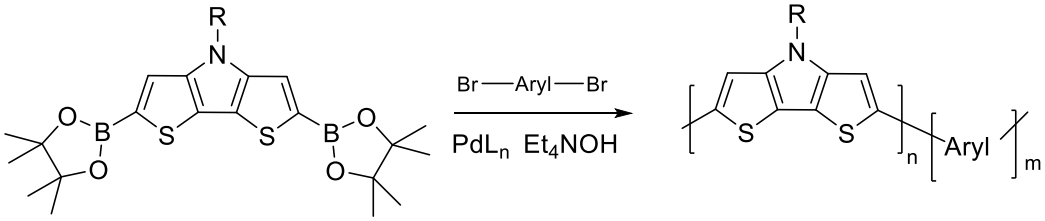

Scheme 1.4.5: Polymerization by Suzuki polycondensation

The publication of Qin is noteworthy not only as the first example of soluble DTP copolymers, but also for having reported the first polycondensation via Suzuki. These initial studies opened a new unexplored field, therefore a wide variety of alternating DTP-based copolymeric materials have been reported. In the recent years a new class of DTP based copolymers has been generated. Several research groups tried the combination of DTP with a trimeric unit, most typically a dithienyl-capped acceptor, in order generate multi-component alternating copolymeric materials (Figure 1.4.2).[49,50,51,52]

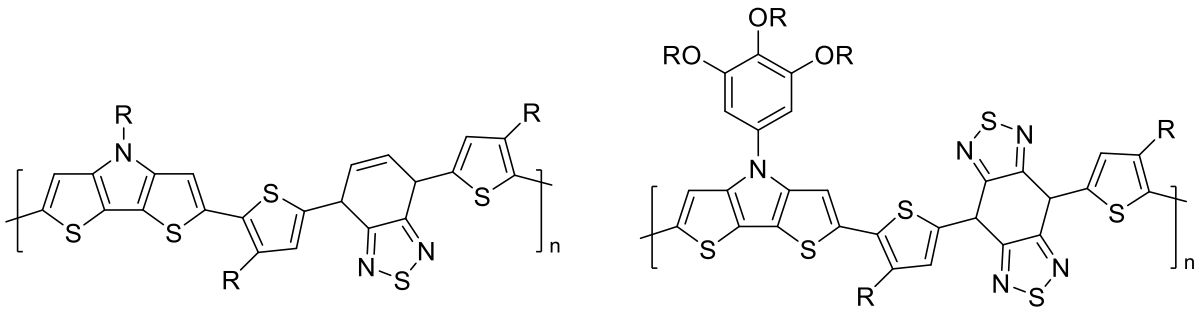

Figure 1.4.2: Example of multi-component DTP based polymer

The formation of the polymer proceeds via either Stille, Suzuki cross-coupling, or dibromination of the trimeric unit by treatment with NBS, and then copolymerization with a distannylDTP via Stille cross-coupling, as reported in Figure 1.4.3.[49,50,53,54]

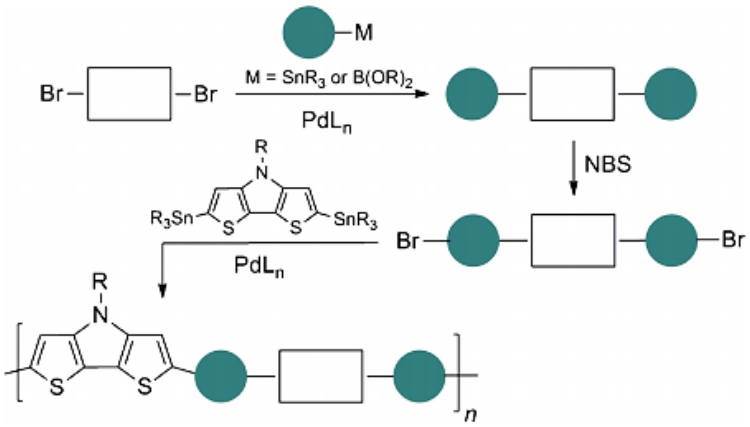

Figure 1.4.3: General synthetic route to multi-component DTP based copolymers

1.4.3 Properties

First generation

The electronic and optical properties of PDTP derivates, as well as for any conjugated polymer, depend on E_g: the number of conjugated double bonds, presence of cycles, and the structural rigidity have an influence on the band gap. The first studies were conducted on first generation oligomers. Regarding optical proprieties, an absorption red shifted of 5 – 15 nm, in comparison with the thiophene derivate, was observed.[55,56,57,58,59] This is probably due to the increased planarity as result of the fused ring typical of DTP monomer.[4] Moreover, further investigation showed that the majority of oligomers exhibited relatively strong solution fluorescence, with quantum yields 2–4 times greater than those of the parent oligothiophenes. This increased emission has been attributed to the photochemical stability of the DTP unit, combined with a decrease in non-radiative vibrations thanks the presence of the fused-ring; in the derivate polymers, fluorescence is still observable with quantum efficiencies as high as 34%.[42]

Dithienopyrrole functionalized with a chiral side chain can show chiroptical activity. The PDTP is to be able to change the supramolecular structure based on the chiral substituent used. PDTP with an alkyl substituent, stack as a series of tilted chains, resulting in an helical structure.[13] Indeed, it is clear that the optical activity of the polymers is deeply influenced by the side chain, as reported by Koeckelberghs and coworkers.[41,13] Side chains can promote

secondary interactions (hydrogen bonding, solvophobic interaction, π stacking, ione pair repulsion and chalcogen-chalcogen interaction) helping the stacking of the polymer chains. This happens in particular with branched alkyl groups.[60] In contrast, with moieties as tri(alkyl)-substituted gallic acid, the presence of space confinement, π-stacking and van der Waals interactions favors a helical conformation.[61]

Several investigations were also done around the band gap: *N*-alkyl homopolymer, reported by Zotti and coworkers in the 1992, exhibited a band gap of ∼1.7 eV and in situ conductivity was 40 S cm^{-1}.[38] In particular, it was observed that the *N*-alkyl derivate displayed a smaller band gap and higher conductivity than the unfunctionalized parent polyDTP. A new investigation was reported in 2002 by Rasmussen and coworkers but the polyDTP characterized had a low yield of high molar mass polymer.[39,42,43] The resulting soluble materials exhibited band gaps from 1.6 to 1.8 eV, similar to the value observed by Zotti. As supported also by the DTP oligomeric series reported by Roncali and coworkers, probably higher molar mass materials exhibits higher conjugation lengths and further reduces E_g values.[56]

The behavior observed for DTP homopolymers, was reported also for DTP-arylene copolymers. The materials exhibit a strong fluorescence with quantum yields around 55.5% in solution and 25.5% in the solid state.[48,62] The fluorescence reported here is the highest quantum yield for thiophene based polymers. In addition to the simple DTP-arylene and DTP thiophene copolymers discussed above, the copolymer can be used to build donator-acceptor copolymers. This polymerization proceeds via Stille cross coupling of distannylated DTP, in the same way as the majority of copolymerization. Fundamental to obtain high molar mass, is the purity of the distannylDTP intermediate.[59] Regarding the optical and electronic properties for the alternating DTP-acceptor copolymers, they exhibit a red shift due to the charge transfer (CT) nature of the HOMO–LUMO transition in these materials. The band gap was also quite reduced in comparison with the PDTP material derivate, (i.e. $E_g < 1.5$ eV). It was observed that in this kind of copolymer, the significant differences in molecular weights cause large effects on the resulting electronic properties of the material. In materials with comparable M_n, the properties were essentially independent from the side chain.[63] However, it was verified that polymers with lower M_n values showed an increase in band gap (∼1.5 eV)

and a stabilization of the HOMO.[64] Differently, materials with significantly larger M_n values result in reduction of the E_g to 1.2 eV and destabilization of the HOMO. [65]

Different electronic and optical properties have been observed during the analysis of multi-component DTP-based copolymers. The resulting band gaps were lower than DTP homopolymers and E_g value is commonly below 1 eV. In comparison to the previously discussed materials, these copolymers exhibit lower band gaps, due to the application of strong acceptors that stabilize LUMO levels. A different structure was analyzed by Janssen and coworkers, who synthetized a multi component of DTP with a spacer between this molecule and the acceptor unit.[66] In this condition the use of an alkyne spacer resulted in higher band gap in comparison to the analogous material.

Despite the fact that not a lot has been reported concerning second generation PDTPs, a significantly red shift absorption and bound gap of 1.60 eV was found in some examples.[39] In that way, like the first generation, the second generation polymer shows a band low enough that the electrons can pass from neutral state to excited state easily by thermal and photo-excitement. This lower band gap can contribute to stabilization of the doped or oxidized state.[39]

1.4.5 Applications

One of the earliest applications of DTP-based materials was their use in field-effect transistor devices (OFETs). The field effect is a phenomenon in which the conductivity of a semiconductor changes due to the application of an electric field normal to its surface. OFETs are composed of three terminals, the source, drain, and gate: an insulator layer separates the semiconductive layer and the gate. (Figure 1.4.4) The semiconductor layer is connected to the drain and source. The electric field is applied via the metallic gate in this device, in that way holes are accumulated at the interface between semiconductor and insulator. The increased charge carrier density causes a highly conductive channel to open between the source and the drain. The transistor is switched on and a current can be driven between source and drain. The semiconductor is usually a planar molecule with aromatics rings and polytiophene derivates are one of the major categories. Ordered stacking of π-conjugated molecules leads to maximum carrier mobility along the direction of stacking, yielding optimal performance.

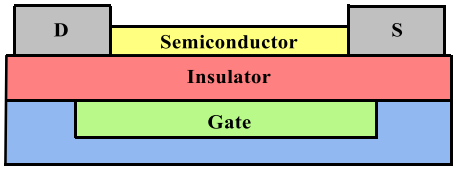

Figure 1.4.4: Organic field-effect transistor device

Due to solid-state emission efficiencies, DTP based materials could also use as emitting compound in organic light-emitting diode (OLED), i.e a light-emitting diode (LED) in which the emissive electroluminescent layer is an organic compound that emits light in response to an electric current. Patri and coworkers reported a first application of DTP in emitting layer of OLED (red) in 2009.[52] In the next year, devices with homopolymers and copolymers, which give a colorful emission were investigated. The organic devices are composed of different components (Figure 1.4.5);

- substrate layer: it supports the OLED and is made up of transparent plastic or glass film;
- anode layer: it is a transparent layer where holes are formed. Indium tin oxide (ITO) is commonly used as the anode material;
- hole transport layer: transports holes from anode. Made up of organic material;
- emissive layer: it is made up of organic plastic and it is responsible of the emission;
- electron transport layer: transports electron from cathode;
- cathode layer: electrons are generated here. It may be transparent or not. Metals such as aluminium and calcium are often used in the cathode;

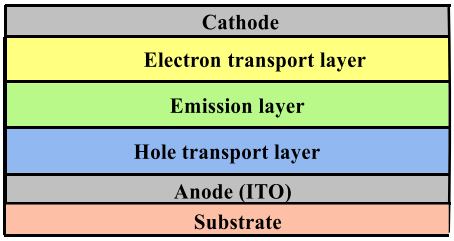

Figure 1.4.5: OLED structure

DTP monomers are also used in bulk heterojunction organic photovoltaics devices (BJH OPV). In the earliest reports these polymers did not have a sufficient quality to produce working devices, due to the low solubility and small molar mass nature of the polymers.[4] The limitations of low molar mass and poor solubility can be overcome by the incorporation of DTP units into a copolymeric material and a wide variety of such copolymeric materials have since been utilized as donor materials in BHJ OPV devices. Typical BHJ OPV cells are shown schematically in Figure 1.4.2 along with the energetic levels involved in charge generation/transport. In these devices, a glass or plastic substrate is coated with ITO as the transparent anode. The photoactive layer is sandwiched between the anode and the top low work function cathode, typically Al or Ca. Interfacial layers can be inserted between the anode-photoactive and cathode-photoactive layers to improve device performance and stabilize operation (Figure 1.4.6).[67,68]

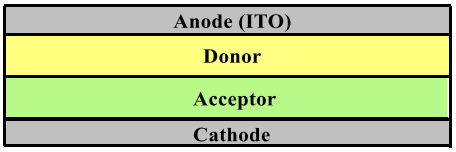

Figure 1.4.6: Organic photovoltaic system

1.5 Bibliography

1. Coakley, K. M. & McGehee, M. D. Conjugated polymer photovoltaic cells. *Chemistry of Materials* **16,** 4533–4542 (2004).

2. Hilberer, A. *et al.* Photonic Materials for Electroluminescent, Laser and Photovoltaic Devices. *Macromol. Symp.* **1**, 99–109 (1997).

3. Moliton, A. & Hiorns, R. C. Review of electronic and optical properties of semiconducting-conjugated polymers: Applications in optoelectronics. *Polym. Int.* **53,** 1397–1412 (2004).

4. Rasmussen, S. C. Electrically conducting plastics: Revising the history of conjugated organic polymers. in *ACS Symposium Series* **1080,** 147–163 (2011).

5. Hideki, S., Louis, E. J., MacDiarmid, A. G., Chiang, C. K. & Heeger, A. J. Synthesis of Electrically-Conducting organic Polymers: Halogen Derivatives of Polyacetylene, (CH)x. *J.C.S., Chem. Commun.* **0**, 1–5 (1977).

6. Chiang, C. K., Fincher, C. R., Park, Y. W., Heeger, A. J., Shirakawa, H., Louis, E. J., Gau, S. C., MacDiarmi, A G. Electrical conductivity in doped polyacetylene. *Phys. Rev. Lett.* **39,** 1098–1101 (1977).

7. Chiang, C. K., Park, Y. W., Heeger, A. J., Shirakawa, H., Louis, E. J., MacDiarmid, A. G. Conducting polymers: Halogen doped polyacetylene. *J. Chem. Phys.* **69,** 5098 (1978).

8. Kobilka, B. M. & Jeffries-el, M. Evaluating chalcogen heteroatoms in conjugated polymers for organic electronics. (2013).

9. Brocks, G. & Tol, A. A theoretical study of polysqueraines. *Synth. Met.* **76,** 213–216 (1996).

10. Van Mullekom, H. A. M., Vekemans, J. A. J. M., Havinga, E. E. & Meijer, E. W. Developments in the chemistry and band gap engineering of donor-acceptor substituted conjugated polymers. *Mater. Sci. Eng. Reports* **32,** 1–40 (2001).

11. Rasmussen, S. C. & Evenson, S. J. Dithieno[3,2-b:2′,3′-d]pyrrole-based materials: Synthesis and application to organic electronics. *Prog. Polym. Sci.* **38,** 1773-1804 (2013).

12. Zhang, Z. B., Motonaga, M., Fujiki, M. & McKenna, C. E. The first optically active polycarbazoles. *Macromolecules* **36,** 6956–6958 (2003).

13. Vanormelingen, W., Van Den Bergh, K., Verbiest, T. & Koeckelberghs, G. Conformational transitions in chiral, gallic acid-functionalized poly(dithienopyrrole): A comparative UV-vis and CD study. *Macromolecules* **41,** 5582–5589 (2008).

14. Goto, H., Okamoto, Y. & Yashima, E. Metal-induced supramolecular chirality in an optically active polythiophene aggregate. *Chem. - A Eur. J.* **8,** 4027–4036 (2002).

15. Vanormelingen, W. *et al.* Conformational steering in substituted poly(3,6-phenanthrene)s: A linear and nonlinear optical study. *Macromolecules* **42,** 4282–4287 (2009).

16. Verswyvel, M. & Koeckelberghs, G. Chirality in conjugated polymers: when two components meet. *Polym. Chem.* **3,** 3203–3216 (2012).

17. Ciardelli, F., Lanzillo, S. & Pieroni, O. Optically Active Polymers of 1-Alkynes. *Macromolecules* **7,** 174–179 (1967).

18. Lemaire, M., Delabouglise, D., Garreau, R., Guy, A. & Roncali, J. Enantioselective chiral poly(thiophenes). *J. Chem. Soc. Chem. Commun.* **12**, 658 (1988).

19. Green, M. M. *et al.* Macromolecular stereochemistry: the out-of-proportion influence of optically active comonomers on the conformational characteristics of polyisocyanates. The sergeants and soldiers experiment. *J. Am. Chem. Soc.* **111,** 6452–6454 (1989).

20. Van den Bergh, K., Huybrechts, J., Verbiest, T. & Koeckelberghs, G. Transfer of Supramolecular Chirality in Block Copoly(thiophene)s. *Chem. - A Eur. J.* **14,** 9122–9125 (2008).

21. Zheng, C. *et al.* Relationships between main-chain chirality and photophysical properties in chiral conjugated polymers. *J. Mater. Chem. C* **2,** 7336–7347 (2014).

22. Szwarc, M., Levy, M. & Milkovich, R. Polymerization initiated by electron transfer to monomer. A new method of formation of block polymers. *J. Am. Chem. Soc.* **78,** 2656–2657 (1956).

23. Halasa, A. F. Recent advances in anionic polymerization. *Rubber Chemistry and Technology* **54,** 627–640 (1981).

24. Moad, G. & Solomon, D. H. *The Chemistry of Radical Polymerization*. *The Chemistry of Radical Polymerization* **23**, 5748–5764 (2005).

25. Bryan, Z. J. & McNeil, A. J. Conjugated polymer synthesis via catalyst-transfer polycondensation (CTP): Mechanism, scope, and applications. *Macromolecules* **46,** 8395–8405 (2013).

26. Sheina, E. E., Liu, J., Lovu, M. C., Laird, D. W. & McCullough, R. D. Chain growth mechanism for regioregular nickel-initiated cross-coupling polymerizations. *Macromolecules* **37,** 3526–3528 (2004).

27. Yokoyama, A., Miyakoshi, R. & Yokozawa, T. Chain-Growth Polymerization for Poly(3-hexylthiophene) with a Defined Molecular Weight and a Low Polydispersity. *Macromolecules* **37,** 1169–1171 (2004).

28. Tamao, K. *et al.* Nickel-Phosphine Complex-Catalyzed Grignard Coupling. I. Cross-Coupling of Alkyl, Aryl, and Alkenyl Grignard Reagents with Aryl and Alkenyl Halides: General Scope and Limitations. *Bulletin of the Chemical Society of Japan* **49,** 1958–1969 (1976).

29. Huddleston, N. E., Sontag, S. K., Bilbrey, J. A., Sheppard, G. R. & Locklin, J. Palladium-mediated surface-initiated Kumada catalyst polycondensation: A facile route towards oriented conjugated polymers. *Macromol. Rapid Commun.* **33,** 2115–2120 (2012).

30. Koeckelberghs, G., Hardeman, T., Van Den Eede, M.-P. & Verheyen, L. Controlled

synthesis of conjugated polymers and block copolymers. *Polymer* **108**, 97–132 (2016).

31. Wu, S., Huang, L., Tian, H., Geng, Y. & Wang, F. LiCl-promoted chain growth kumada catalyst-transfer polycondensation of the 'reversed' thiophene monomer. *Macromolecules* **44,** 7558–7567 (2011).

32. Lamps, J. P. & Catala, J. M. Kinetic study, by UV-vis spectroscopy, on the strong effect of LiCl on the controlled polymerization of 2-bromo-3-hexyl-5-iodothiophene and 2-iodo-3-hexyl-5-bromothiophene: Determination of the propagation rate constants, application to the synthesis of high Molecular Weight Polydodecylthiophene. *Macromolecules* **44,** 7962–7968 (2011).

33. Fodor, Z., Kennedy, J. P., Kelen, T. & Tudos, F. Quasiliving carbocationic polymerization. XVIII. Synthesis of poly(styrene-β -isobutylene-β -styrene). *J. Macromol. Sci. Chem.* **A24,** 735–747 (1987).

34. Higashimura, T., Teranishi, H. & Sawamoto, M. Living Cationic Polymerization of N-Vinylcarbazole with Iodine. *Polymer Journal* **12,** 393–398 (1980).

35. Bonillo, B. & Swager, T. M. Chain-Growth Polymerization of 2 - Chlorothiophenes Promoted by Lewis Acids. *J. Am. Chem. Soc* **134,** 18916–18919 (2012).

36. Olah, G. A. George A. Olah. *Angew. Chem. Int. Ed.* **52,** 8500–8500 (2013).

37. Zanirato, P., Spagnolo, P., Zanardi, G. Thermal decomposition of oazidobithienyls. *J Chem Soc Perkin Trans* **1**, 2551–2254 (1983)

38. Zotti, G., Schiavon, G., Berlin, A. & Pagani, G. Electrochemical polymerization of 3-alkylthiopyrroles. *Synth. Met.* **28,** 183–186 (1989).

39. Evenson, S. J. & Rasmussen, S. C. N-Acyldithieno 3,2-b:2 ',3 '-d pyrroles: Second Generation Dithieno 3,2-b:2 ',3 '-d pyrrole Building Blocks with Stabilized Energy Levels. *Org. Lett.* **12,** 4054–4057 (2010).

40. Koeckelberghs, G. *et al.* Improved synthesis of N-alkyl substituted dithieno[3,2-b:2′,3′-d]pyrroles. *Tetrahedron* **61,** 687–691 (2005).

41. Koeckelberghs, G., Cremer, L. De & Verbiest, T. Influence of the Substituent and Polymerization Methodology on the Properties of Chiral Poly (dithieno [3 , 2-b : 2 ′, 3 ′ -d] pyrrole) s. *Macromolecules* **40,** 4173–4181 (2007).

42. Rasmussen, S. C., Kenning, D. D., Ogawa, K., Rothstein, S. D. & Seth, C. Nitrogen-Derivatized Polythiophenes: Polythieno[3,4-b]pyrazines, Polyaminothiophenes, and Polythienopyrroles 3–5 *Polymeric Materials: Science & Engineering* **86**, 59 (2002).

43. Ogawa, K., Stafford, J. A., Rothstein, S. D., Tallman, D. E. & Rasmussen, S. C. Nitrogen-functionalized polythiophenes: Potential routes to new low band gap materials. in *Synthetic Metals* **152,** 137–140 (2005).

44. Koeckelberghs, G. *et al.* Improved synthesis of N-alkyl substituted dithieno[3,2-b:2′,3′-d]pyrroles. *Tetrahedron* **61,** 687–691 (2005).

45. Bronstein, H. A. & Luscombe, C. K. Externally initiated regioregular P3HT with controlled molecular weight and narrow polydispersity. *J. Am. Chem. Soc.* **131,** 12894–12895 (2009).

46. Casalbore-Miceli, G., Beggiato, G., Zotti, G. & Favaretto, L. Electrochemical preparation of the thionaphtheneindole-dithienopyrrole copolymer. *Synth. Met.* **68,** 85–89 (1994).

47. Beggiato, G., Casalbore-Miceli, G., Geri, A., Berlin, A. & Pagani, G. Electrochemical preparation and electrochromic characteristics of dithienopyrrole-dithienothiophene, dithienopyrrole-thionaphtheneindole and dithienothiophene-thionaphtheneindole copolymers. *Synth. Met.* **82,** 11–15 (1996).

48. Zhang, W., Li, J., Zhang, B. & Qin, J. Highly Fluorescent Conjugated Copolymers Containing Dithieno[3,2- b :2′,3′- d]pyrrole. *Macromol. Rapid Commun.* **29,** 1603–1608 (2008).

49. Steckler, T. T. *et al.* A Spray-Processable, Low Bandgap, and Ambipolar Donor−Acceptor Conjugated Polymer. *J. Am. Chem. Soc.* **131,** 2824–2826 (2009).

50. Zhou, E., Tajima, K., Yang, C. & Hashimoto, K. Band gap and molecular energy level

control of perylene diimide-based donor–acceptor copolymers for all-polymer solar cells. *J. Mater. Chem.* **20,** 2362 (2010).

51. Shi, M. M. *et al.* Design and synthesis of dithieno[3,2-b:2′3′-d]pyrrole-based conjugated polymers for photovoltaic applications: Consensus between low bandgap and low HOMO energy level. *J. Polym. Sci. Part A Polym. Chem.* **49,** 1453–1461 (2011).

52. Mishra, S. P., Palai, A. K., Srivastava, R., Kamalasanan, M. N. & Patri, M. Dithieno[3,2-b:2′,3′-d]pyrrole-Alkylthiophene-Benzo[1,2,5]thiadiazole-based highly stable and low band gap polymers for polymer light-emitting diodes. *J. Polym. Sci. Part A Polym. Chem.* **47,** 6514–6525 (2009).

53. Zhou, E., Cong, J., Tajima, K., Yang, C. & Hashimoto, K. Synthesis and photovoltaic properties of donor-acceptor copolymer based on dithienopyrrole and thienopyrroledione. *Macromol. Chem. Phys.* **212,** 305–310 (2011).

54. Ahmed, E., Subramaniyan, S., Kim, F. S., Xin, H. & Jenekhe, S. A. Benzobisthiazole-based donor-acceptor copolymer semiconductors for photovoltaic cells and highly stable field-effect transistors. *Macromolecules* **44,** 7207–7219 (2011).

55. Wong, H. L., Ko, C. C., Lam, W. H., Zhu, N. & Yam, V. W. W. Design and synthesis of a new class of photochromic diarylethenecontaining dithieno[3,2-b:2’,3’-d]pyrroles and their switchable luminescence properties. *Chem. - A Eur. J.* **15,** 10005–10009 (2009).

56. Yassin, A., Leriche, P. & Roneali, J. Synthesis and chain-length dependence of the electronic properties of π-conjugated dithieno[3,2-b:2′,3′-d]pyrrole (DTP) oligomers. *Macromol. Rapid Commun.* **31,** 1467–1472 (2010).

57. Barlow, S. *et al.* Electronic and optical properties of 4H-cyclopenta[2,1-b:3,4-b’]bithiophene derivatives and their 4-heteroatom-substituted analogues: a joint theoretical and experimental comparison. *J. Phys. Chem. B* **114,** 14397–407 (2010).

58. Evenson, S. J. *et al.* Molecular tuning in highly fluorescent dithieno[3,2-b:2’,3’-

d]pyrrole-based oligomers: effects of N-functionalization and terminal aryl unit. *Phys. Chem. Chem. Phys.* **14,** 6101–11 (2012).

59. Mo, H. *et al.* Solution and solid-state properties of highly fluorescent dithieno[3,2-b:2',3'-d]pyrrole-based oligothiophenes. *Phys. Chem. Chem. Phys.* **12,** 14585–14595 (2010).

60. Cheuk, K. K. L., Lam, J. W. Y., Chen, J., Lai, L. M. & Tang, B. Z. Amino acid-containing polyacetylenes: Synthesis, hydrogen bonding, chirality transcription, and chain helicity of amphiphilic poly(phenylacetylene)s carrying L-leucine pendants. *Macromolecules* **36,** 5947–5959 (2003).

61. Lai, L. M. *et al.* Optically active polyacetylene: Synthesis and helical conformation of a poly(phenylacetylene) carrying L-alanyl-L-alanine pendants. *J. Polym. Sci. Part A Polym. Chem.* **43,** 3701–3706 (2005).

62. Evenson, S. J., Mumm, M. J., Pokhodnya, K. I. & Rasmussen, S. C. Highly fluorescent dithieno[3,2-b:2′,3′-d]pyrrole-based materials: Synthesis, characterization, and OLED device applications. *Macromolecules* **44,** 835–841 (2011).

63. Yue, W. *et al.* Novel NIR-absorbing conjugated polymers for efficient polymer solar cells: effect of alkyl chain length on device performance. *J. Mater. Chem.* **19,** 2199 (2009).

64. Price, S. C., Stuart, A. C. & You, W. Polycyclic aromatics with flanking thiophenes: Tuning energy level and band gap of conjugated polymers for bulk heterojunction photovoltaics. *Macromolecules* **43,** 797–804 (2010).

65. Zhang, S. M. *et al.* Low Bandgap pi-Conjugated Copolymers Based on Fused Thiophenes and Benzothiadiazole: Synthesis and Structure-Property Relationship Study. *J. Polym. Sci. Part a-Polymer Chem.* **47,** 5498–5508 (2009).

66. Ashraf, R. S., Gilot, J. & Janssen, R. A. J. Fused ring thiophene-based poly(heteroarylene ethynylene)s for organic solar cells. *Sol. Energy Mater. Sol. Cells* **94,** 1759–1766 (2010).

67. Hotchkiss, P. J. *et al.* The Modification of Indium Tin Oxide with Phosphonic Acids: Mechanism of Binding, Tuning of Surface Properties, and Potential for Use in Organic Electronic Applications. *Acc. Chem. Res.* **45,** 337–346 (2012).

68. Facchetti, A. Polymer donor-polymer acceptor (all-polymer) solar cells. *Materials Today* **16,** 123–132 (2013).

CHAPTER 2: AIM OF THE PROJECT

Polydithienopyrrole (PDTP) offers many advantages compared to common polymers in organic electronics. Its structure permits good electronic conjugation and stable oxidation state. The monomer has also different reactive centers, which makes it easy to derivatize. Dithienopyrrole (DTP) derivates were polymerized since 1950. Despite that, the controlled polymerization is still not completely explored. The possibility to control molar mass and termination of the growing chain is fundamental to create well-defined, reproducible materials. For this reason, in order to apply PDTP as organic conjugated polymer, the possibility of controlled polymerization needs to be verified. Another aspect that is still not completely explored is bound to the optical activity of the PDTP, which bearing appropriate substituents may adopt a helical conformation. The configuration of the helix, built up from achiral co-monomers, can be established in an enantiopure way by using only a small percentage of the chiral monomer co-polymerized with achiral co-monomer. The effect, called "sergeants and soldiers effect", is expressed by the nonlinear increase of the chiral response vs the ratio of the chiral co-monomer used for the polymerization. To date, this effect is still not completely explored for PDTP.

This project will investigate, firstly the possibility to obtain a controlled polymerization of PDTP. Then, monomers with different side chains and organometallic functions will be screened for a CTCP-type polymerization. Also a Lewis-acid based cationic polymerization will be performed. Moreover the chemical derivatization of DTP is explored: the research is going to concern also block copolymers, built up by DTP and monomers of different nature.

The research will be extended also to the investigation of optically active derivates of PDTP, using a chiral monomer for the synthesis. The possibility to develop a supramolecular distribution of the polymeric chains, together with the "sergeant and soldiers effect" will be checked investigating a series of polymers with increasing amounts of chiral monomer.

CHAPTER 3: RESULTS AND DISCUSSION

3.1 Kumada Catalyst Transfer Condensative Polymerization (KCTCP)

The first approach, based on the good result obtained by Miyakoshi, Yokoyama, and Yokozawa in the controlled synthesis of poly(3-hexylthiophene), was to synthetize *N*-dodecyl-2-bromo-6-iodo-dithieno[3,2-*b*:2',3'-*d*]pyrrole **2c**.[1] The monomer was prepared following published procedure by double Buchwald-Hartwig reaction, between dodecyl amine and 3,3'-dibromo-2,2'–bithiophene. The reaction was catalyzed by Pd(BINAP) in presence of NaO*t*-Bu in dry toluene (Scheme 3.1.1).[2]

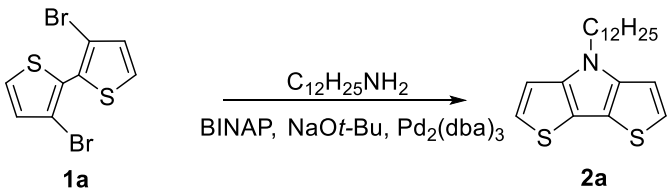

Scheme 3.1.1: Synthesis of 2a

The product wa analyzed by ^{1}H NMR. (Figure 3.1.1)

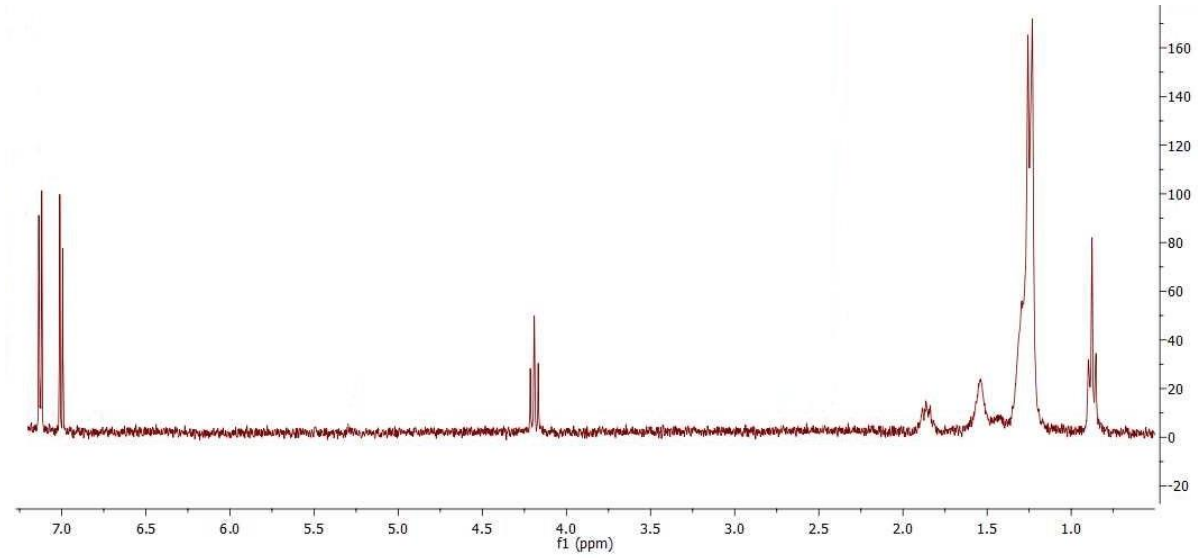

Figure 3.1.1: ^{1}H NMR of 2a

The doublets in the aromatic region, 7.00 ppm (2H) and 7.13 ppm (2H), are ascribed to the protons bound to the thiophenic rings. Regarding the aliphatic region, a triplet is identified at 4.19 ppm as the 2H in alpha to the N atom. From 1.80 ppm until 1.23 ppm, the signals are indistinctly ascribed to the aliphatic chain; at 0.88 a triplet (3H) is identify as CH_3. As previously explained, KCTCP proceeds via coupling of monomers bearing halide and Grignard function. In order to obtain the asymmetric organometallic derivate, the monomer **2a** was brominated and iodinated (Scheme 3.1.2); in this way the different reactivity of the carbon-halogen bond ensured a selective Grignard reaction.[3]

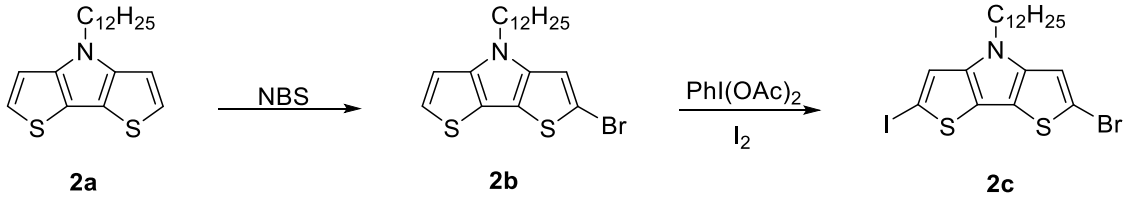

2a **2b** **2c**

Scheme 3.1.2: Synthesis of 2c

The first attempt of synthesis failed: after bromination, the crude compound **2b** polymerized spontaneously even if it was kept under inert atmosphere. The monomer was synthetized over and stored at -18 °C but the uncontrollable polymerization persisted. Despite this, it was possible to purify **2b** by column chromatography from the unreacted and di-brominated compounds. In the next step the product polymerized as soon as the temperature reached 0 °C. Therefore, it was clear that the monomer was extremely unstable due to its electronrich character. Exposing this molecule to temperatures higher than 0°C in presence of light, decomposition and a consequent polymerization were promoted. Considering the iodination not a possible option, the brominated monomer **2b** was reacted with a Knochel-Hauser base (Scheme 3.1.3), forming the organometallic monomer in situ.[4] The reaction was conducted with 2,2,6,6-tetramethylpiperidine MgCl · LiCl in dried THF at -78 °C. After obtaining the Grignard derivate **2d** (not isolated), the polymerization was performed in situ with a solution of 0.01 mmol of 1,3-bis(diphenylphosphino)propane nickel(II) chloride $Ni(dppp)Cl_2$ in dry THF, one of the most widely used catalyst system in controlled synthesis of conjugated polymers.[5]

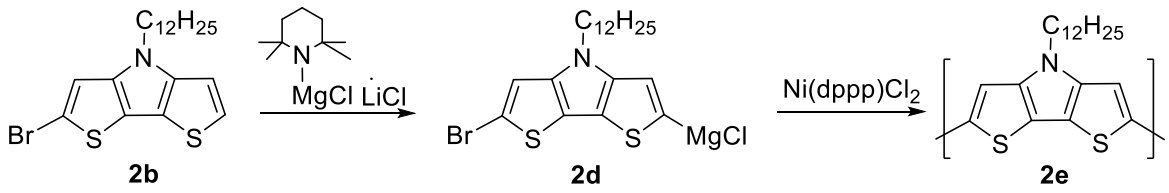

Scheme 3.1.3: Knochel Hauser reaction

The gel permeation chromatogram (GPC) clearly showed that the main products present after the polymerization were trimer and monomer. Mass average molar mass (M_w), number average molar mass (M_n) and polydispersity (Đ) are detailed in Table 3.1.1.

Table 3.1.1: GPC analysis KCTP with Ni based catalyst and 2d

Sample	***Mw [kg/mol]***	***Mn [kg/mol]***	***Đ***
2e	1.8	1.1	1.7

Considering the unstable nature of the molecule, it was decided to synthetize a differently *N*-functionalized DTP. Decreasing the electron density in the brominated intermediate it will be less incline to react with itself, thus we have chosen an aryl amine derivate, 3,4,5-tris(octyloxy)aniline **3c** (Scheme 3.1.4).

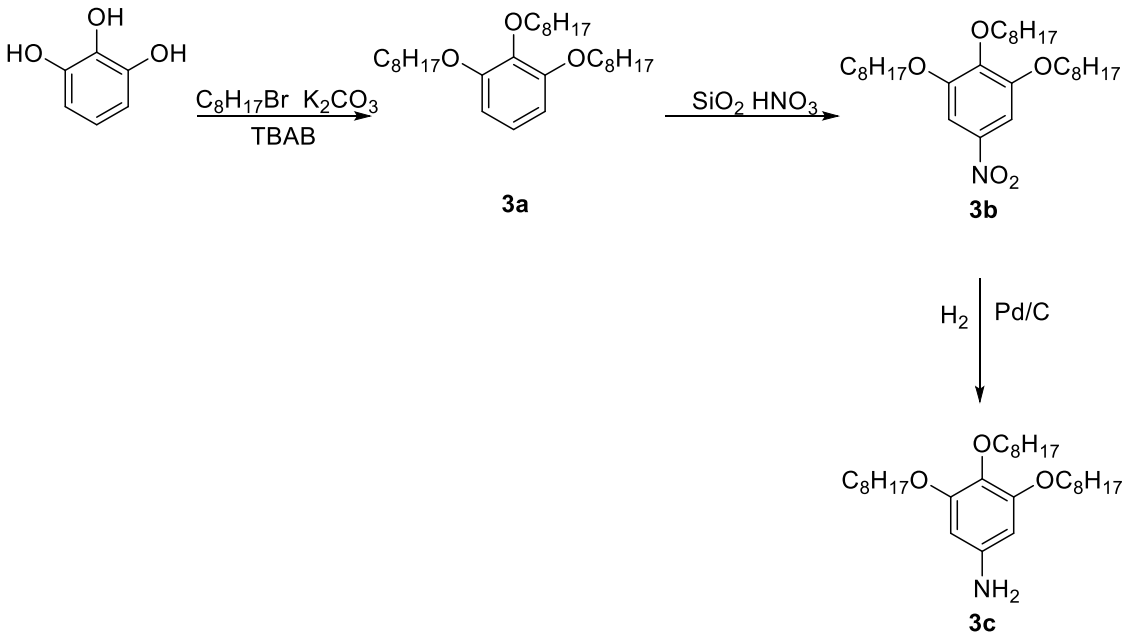

Scheme 3.1.4: Synthesis of 3c

The monomer, *N*-(3,4,5-tri(octyloxy)phenyl)-dithieno[3,2-*b*:2',3'-*d*]pyrrole **4a** (Scheme 3.1.5), was prepared with the same procedure reported but the coupling was conducted between 3,3'-dibromo-2,2'–bithiophene and the 3,4,5-tris(octyloxy)aniline previously prepared.[2]

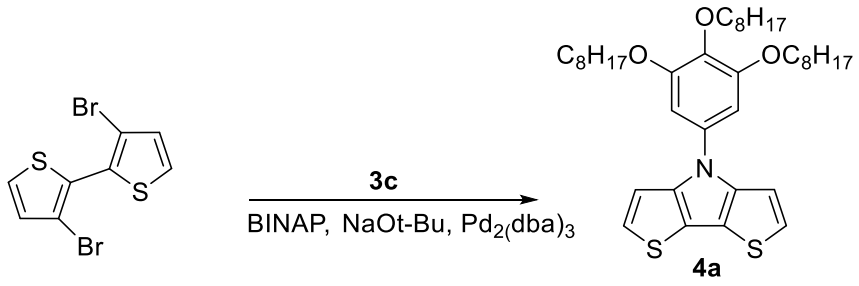

Scheme 3.1.5: Synthesis of 4a

The monomer **4a** was brominated and iodinated (Scheme 3.1.6) for the following KCTCP polymerization.[6]

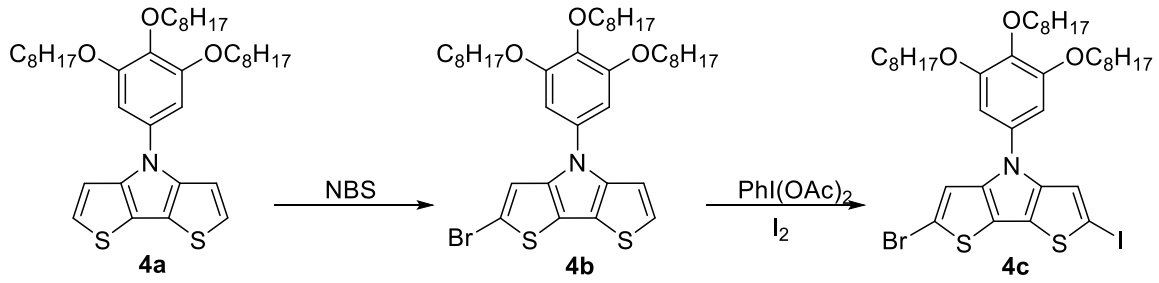

Scheme 3.1.6: Synthesis of 4c

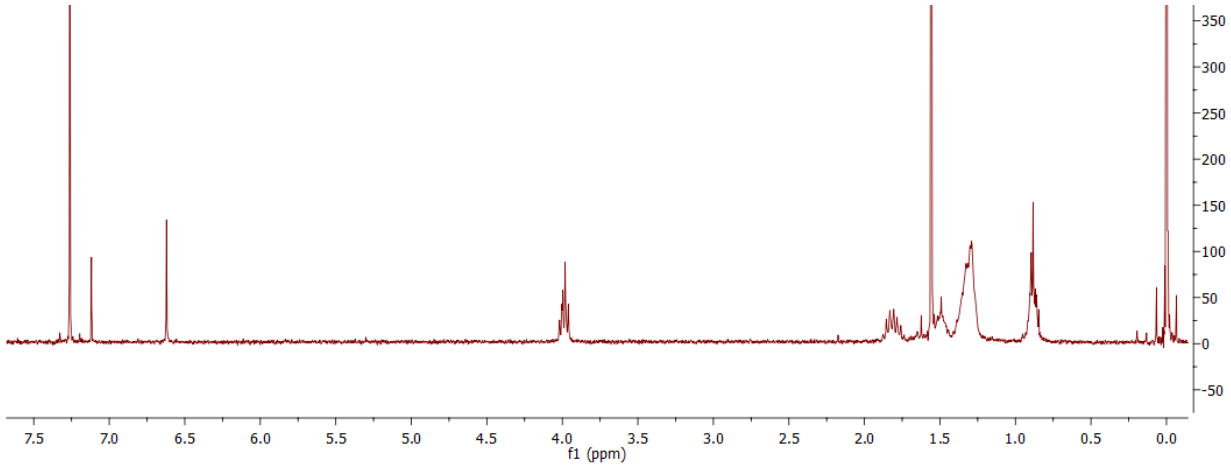

Figure 3.1.2: ^{1}H NMR of 4c

The formation of **4c** was unambiguously confirmed by ^{1}H NMR spectroscopy (Figure 3.1.2).

The ^{1}H NMR spectrum contains signals in the aliphatic region (0.88 ppm – 4.06 ppm), ascribed to the aliphatic chains. The multiplet at 4 ppm (6H) is identified as the CH_2 directly bonded to the oxygen atoms. As regards the aromatic region, the phenyl protons (2H) resonate at 6.62 ppm and appear as a singlet; only one signal at 7.11 ppm (1H) was observed, that was ascribed to one of the two thiophene protons: it is clear that one singlet is missing probably matching with the signal of chloroform.

In order to start the polymerization, the active monomer **4c*** was generated in situ from **4c** via Grignard reaction with 1 equivalent of *i*-PrMgCl·LiCl (Scheme 3.1.7).

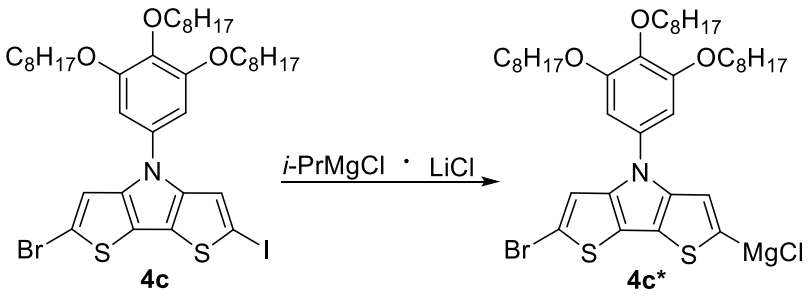

Scheme 3.1.7: Synthesis 4c*

This monomer is stable and does not undergo a spontaneous polymerization. Starting from Ni(dppp)Cl_2, we decided to investigate also [1,3-Bis(diphenylphosphino)propane]dichloro nickel(II) Ni(dppe)Cl_2 and [1,3-Bis(2,6-diisopropylphenyl)imidazol-2-ylidene] triphenylphosphine nickel(II) dichloride Ni(NHC)Cl_2. Indeed by tuning ligands, affecting electronic proprieties or steric hindrance, it is possible to enhance the interaction with the monomer and influence the polymerization. However, GPC spectra showed mostly presence of monomer and dimer for any catalytic system tested (Table 3.1.2).

Table 3.1.2: GPC analysis KCTP with Ni based catalyst and 4c

Catalyst	***Mw [kg/mol]***	***Mn [kg/mol]***	***Đ***
Ni(dppp)Cl_2	2.8	2.5	1.2
Ni(NHC)Cl_2	1.2	0.95	1.3
Ni(dppe)Cl_2	2.7	2.4	1.1

In the light of the above results, the possibility that the absence of polymeric material was not connected to the nature of the ligand was verified. For this reason, a new polymerization in presence of palladium catalyst, (1,3-bis(2,6-diisopropylphenyl)imidazolidene) (3-chloropyridyl) palladium(II) dichloride, PEPPSI Pd was done. Although this metal has a weaker association with the backbone of the molecule, it is still capable of mediating catalyst-associated chain growth polymerization.[7,8,9] The palladium catalyzed polymerization, based on the Neghishi coupling reaction, is done between bromide and organozinc derivate. It is

necessary to convert the organomagnesium monomer **4c** in a zinc derivate by adding $ZnBr_2$.[7] The GPC analysis revealed the same result obtained with Ni – catalysts (Table 3.1.3).

Table 3.1.3: GPC analysis KCTP with Pd based catalyst and 4c

Catalyst	***Mw [kg/mol]***	***Mn [kg/mol]***	***Đ***
PEPPSI Pd	1.5	1.1	1.4

The reactions performed, showed that the problem was not due to the nature of metal or of ligand, therefore we focused on the mechanism of reaction.

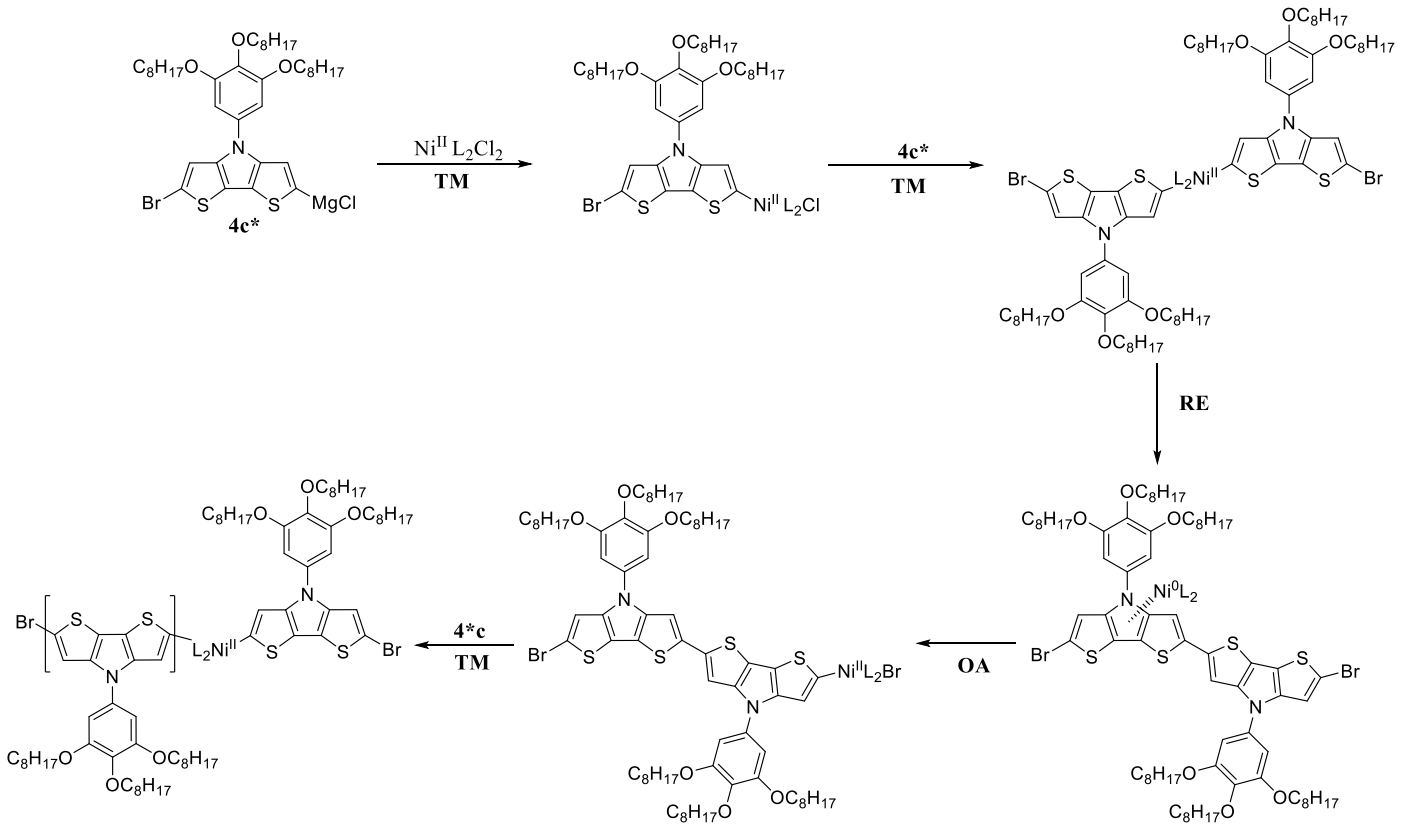

Scheme 3.1.8: Catalytic cycle

The polymerization starts with a double transmetallation (TM) of the monomer on the Ni-species; in that way $Ni^{II}L_2Cl_2$ is reduced (RE), forming the first bond between two monomeric

units. The catalyst (Ni^0) can insert again in the C-Br bond by oxidative addition (OA), continuing the polymerization as reported in Scheme 3.1.8.

It is now clear that if **4c*** is partially or completely not present, the polymerization is hampered. For this reason the correct formation of the Grignard species was checked. The reaction was conducted using 1 equivalent of *i*-PrMgCl: an excess of the organometallic reagent could promote polytermination. The solution was stirred at 0 °C for 20 minutes. The conditions of reaction appeared important, indeed longer time or higher temperature led to side reaction. After quenching a sample before starting the polymerization, the compound was analyzed by H^1 NMR (Figure 3.1.3).

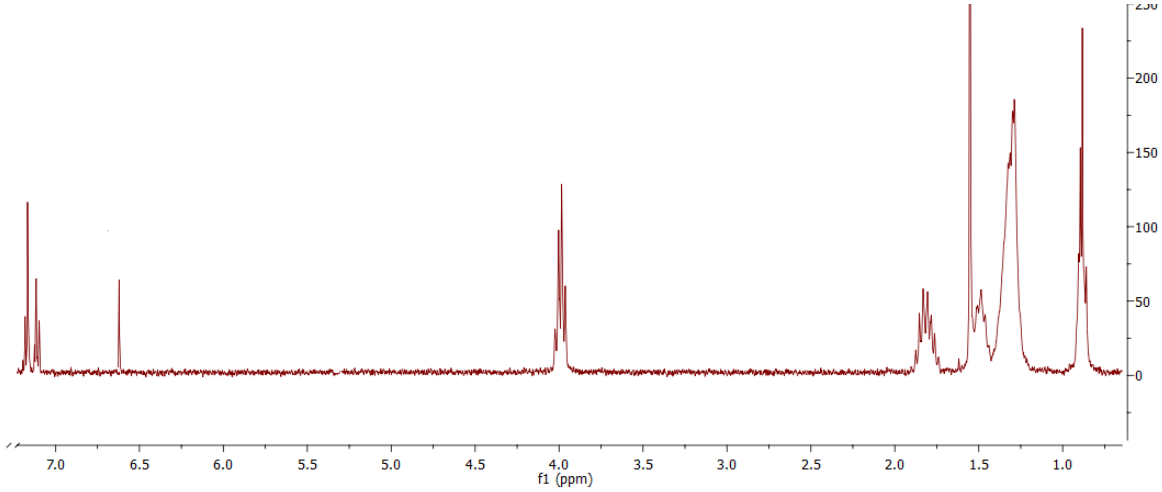

Figure 3.1.3: ^{1}H NMR of protonated 4c*

The ^{1}H NMR data confirmed the presence of protonated **4c*** (7.17 ppm, m, 2H; 7.11 ppm, m, 1H).

The absence of polymeric material could not be ascribed to the formation of the Grignard, therefore we focused on the reactions between the monomer and the catalyst, during the catalytic cycle. The polymerization was then investigated by ^{31}P NMR. We chose to analyze an external initiator, o-tolyl Ni(dppp)Br, synthetized from dppp via ligand exchange. The ^{31}P NMR measurement on the catalyst was then repeated before (Figure 3.1.4a) and after adding **4c*** (Figure 3.1.4b).

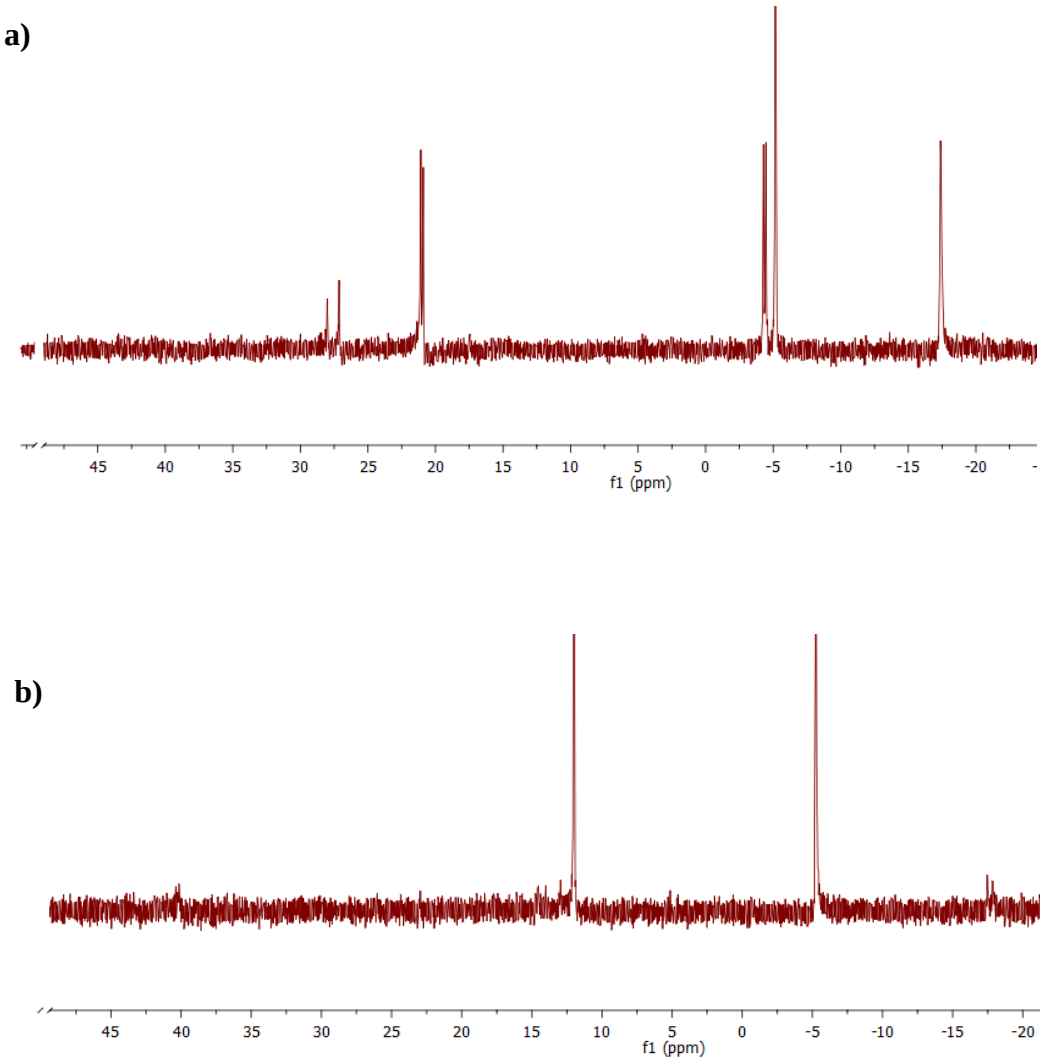

Figure 3.1.4: a) ^{31}P NMR of catalyst before adding 4c*; b) ^{31}P NMR of catalyst after adding 4c*

Before adding the monomer (Figure 3.1.4a), the spectrum contains signals ascribed to the o-tolyl Ni(dppp)Br (21 ppm; -4.44 ppm).[10] The resonance at – 5.23 ppm can be ascribed to free PPh_3 and the one at -17.53 ppm to the dppp.[11,12]

After adding the monomer (Figure 3.1.4b) only two signals are visible: at – 5.23 the peak ascribed to PPh_3 ppm remains visible, while at 12.09 ppm a new singlet is observed. As reported by Bronstein and Luscombe, this signal is caused by a complex of Ni^0, $Ni^0(dppp)_2$.[13] This observation suggest that after reductive elimination, the Ni^0 π-complex is broken and the catalyst is released as Ni(dppp)and it formed a dimer, $Ni(dppp)_2$, with free Ni^0 (Figure 3.1.5).[5]

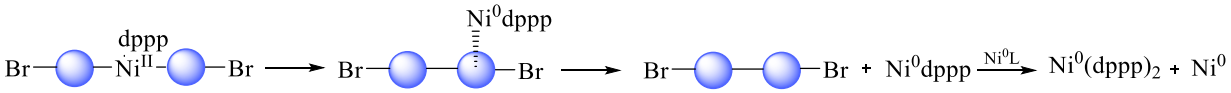

Figure 3.1.5: Mechanism of dissociation

In order to clarify the mechanism, the sample obtained after adding the monomer was analyzed by GPC. The spectrum showed mostly starting material, **4c**, and **4e** (Figure 3.1.6).

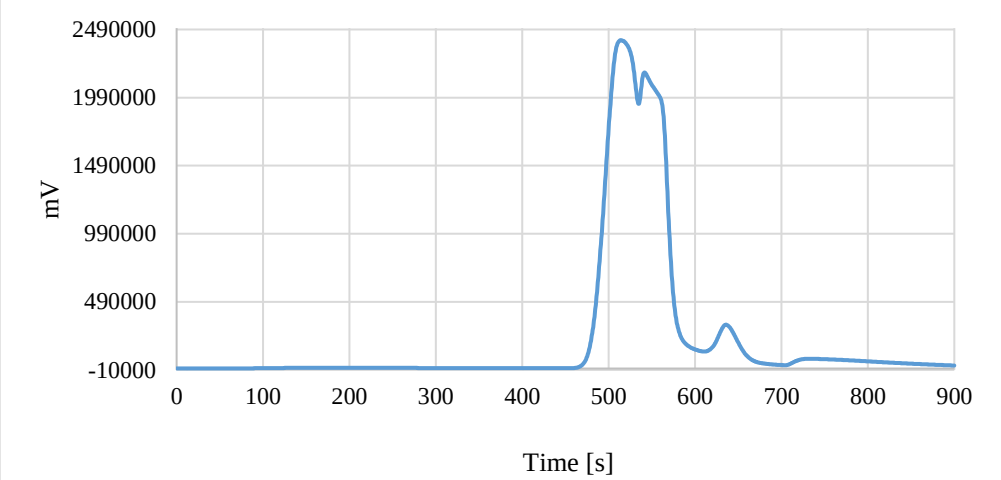

Figure 3.1.6: GPC analysis of the polymerization conducted with o-tolylNi(dppp)Br

It was hypothesized that after transmetallation and reductive elimination, the catalyst was not able to insert again in the C-Br bond; in that way, the polymerization was hampered. We concluded that the catalyst cycle is broken before the OA (Scheme 3.1.9).

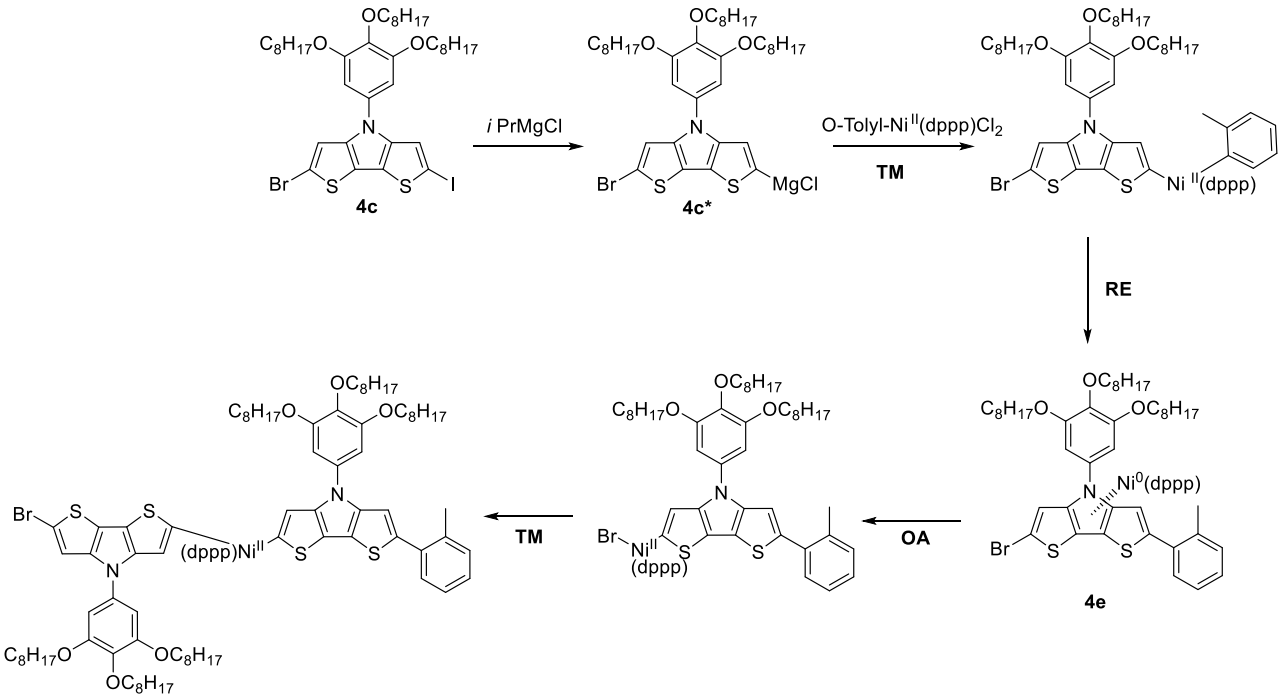

Scheme 3.1.9: KCTCP with external

The OA could fails because:

(1) the complex formed between catalyst and monomer is not strong enough;

(2) the oxidative addition is hampered due to the electron-rich nature of the monomer.

In order to determine the origin of the problem, a test reaction was done. First, it was necessary to verify the interaction between nickel and thiophene; therefore a preliminary reaction was conducted. The thiophefenic alkyl derivate **6a** was reacted with one equivalent of Grignard reagent in presence of Ni(dppp)Cl_2 (Scheme 3.1.10) to determine the necessary reaction condition. If the catalyst stays complexed, it would observe only direacted product; meanwhile if the complexation is too weak, it would observe only monoreacted.

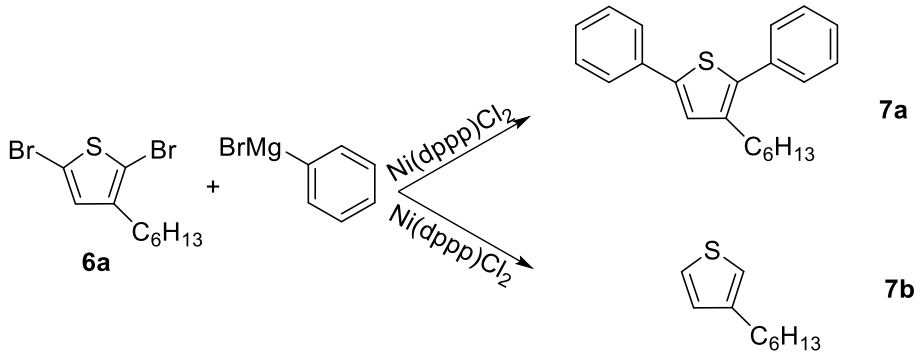

Scheme 3.1.10: Preliminary reaction with 6a and phenyl magnesium bromide

Specifically, the reaction was performed with 1 equivalent of **6a** and 1 of phenyl magnesium bromide. A sample was quenched and analyzed by ^{1}H NMR in order to confirm absence of reaction without catalyst. After that, Ni(dppp)Cl_2 was added and the solution was stirred for 1 hour at room temperature. Unfortunately, the GC/MS spectrum showed the presence of alkyl thiophene **7b**: it was clear that the desired reaction did not occur because the Grignard reaction on the thiophene was faster. In order to slow down the side reaction, the procedure was conducted at 0°C. Despite the different condition, the result did not change. Therefore a different Grignard reagent was used, as reported in Scheme 3.1.11.

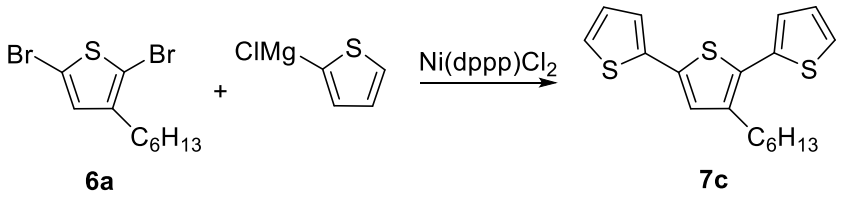

Scheme 3.1.11: Preliminary reaction with 6a and thiophen-2-ylmagnesium chloride

The product was analyzed with GC/MS, confirming the presence of direacted compound; in that way we clearly demonstrated that the reaction with Ni(dppp)Cl_2 was possible in this condition.

The same reaction was conducted with the dibromo DTP derivate **4d** (Scheme 3.1.12).

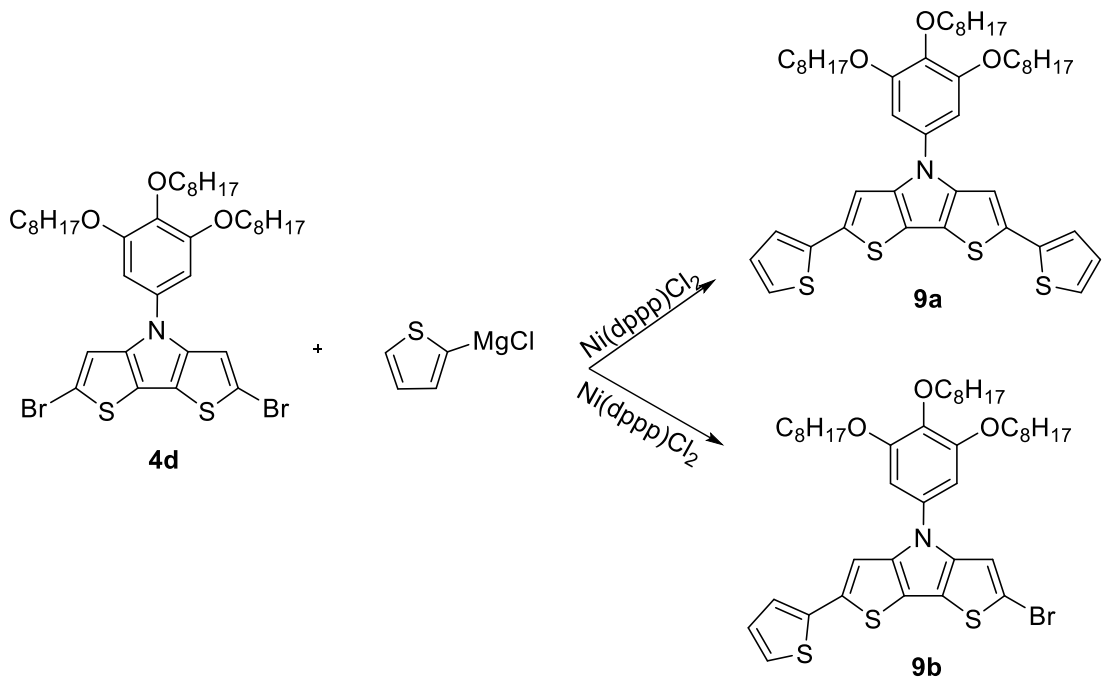

Scheme 3.1.12: Test reaction with 4d and thiophen-2-ylmagnesium chloride

As previously reported, before starting the test reaction, it was necessary to confer the absence of reaction between **4d** and thiophen-2-ylmagnesium chloride. Therefore, the two reagents were added in a dried flask and the solution was stirred for 1 hour at room temperature. The reaction was quenched with water and some drops of HCl (37%). The organic layer was analyzed via ^{1}H NMR, confirming the presence of both the reagents completely unreacted. Then, following what published by Elena E. Sheina and coworkers, the catalyst, Ni(dppp)Cl_2, and **4d** were weighed in the same flask then the Grignard reagent was added at 0°C.[12] The reaction was stirred for 12 hour at RT

If the problem is connected to (1) the complex formed between catalyst and monomer after RE, we should observe the monoreacted product, because Ni^0 is rather reactive and is able to perform OA[1] (Scheme 3.1.13). Otherwise, if we observed the unreacted product, it is evident that the problem is due to the electron-rich nature of the monomer, because not even the first OA[1] takes place (Scheme 3.1.13).

The analysis was attempted with ^{1}H NMR and the resulting spectrum showed mostly presence of starting material **4d**.

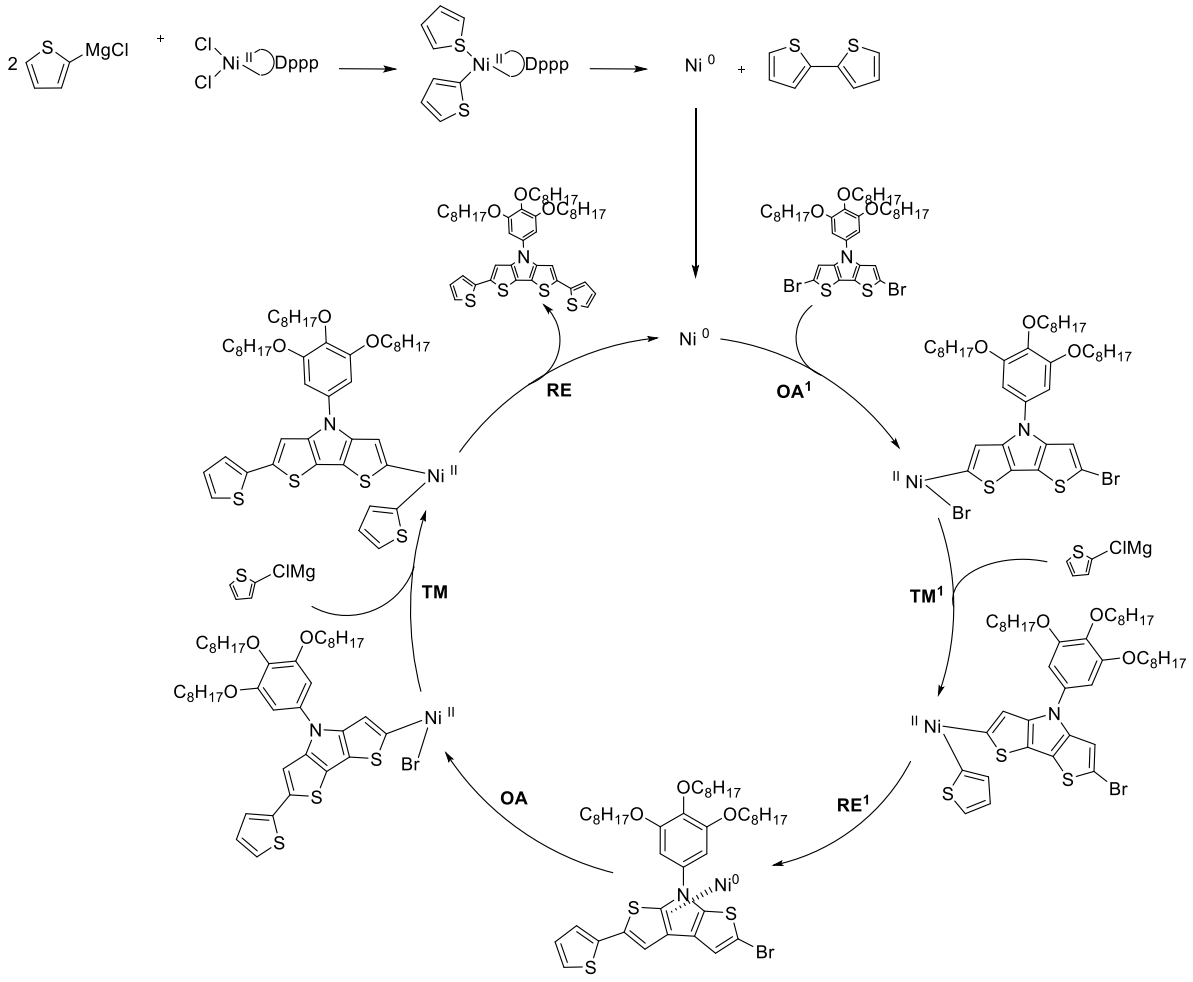

Scheme 3.1.13: Supposed catalytic cycle between 4d and thiophen-2-ylmagnesium chloride

The spectrum obtained was rather complex, since in order to clarify the signals a chromatographic column was taken. In addition to the fraction of **4d** unreacted, it was isolated a small amount of mixture of **9b** and dithiophene (Scheme 3.1.13). Despite this fraction, the most part of the sample was unreacted. For this reason, it was possible to confirm that the polymerization did not occur because the Ni-species was unable to perform the OA^1, due to the electronic nature of the monomer (2). It was concluded to completely change method of polymerization.

3.2 Cationic polymerization catalyzed by acids

Polymerization acid catalyzed is an additional way to perform a controlled product. Good results have been obtained by Bonillo and Swager for the chain growth polymerization of 2-chloro-3-alkoxythiophenes.[14] Based on what was reported, we screened different reaction condition (time, solvent, temperature and Lewis acid) in order to investigate the possibility of controlling the polymerization in our specific case (Scheme 3.2.1).

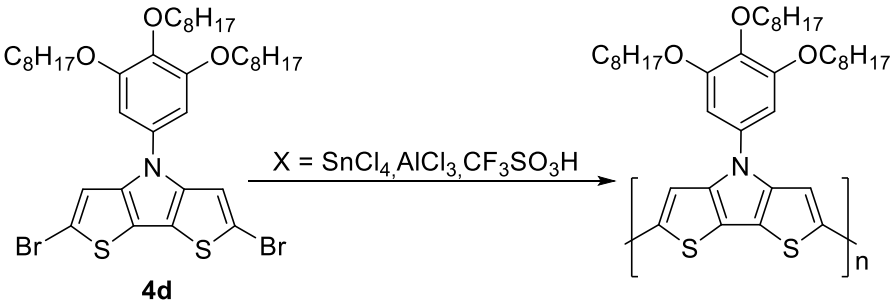

Scheme 3.2.1: Polymerization via Lewis acid

The experimental results are reported in Table 3.2.1.

Table 3.2.1: Results obtained under the different polymerization conditions

Entry	***Lewis acid***	***Solvent***	***% of acid***	***Time***	***T [°C]***	***M_w [kg/mol]***	***M_n [kg/mol]***	***Đ***
1	$SnCl_4$	o-DCB	5	3 days	120	11	6.7	1.6
2	$SnCl_4$ + $SnCl_4$	o-DCB	10	3 days	120	13	4.9	2.6
3	$SnCl_4$	Toluene	5	2 days	80	5.1	4.0	1.3
4	$SnCl_4$ + $SnCl_4$	Toluene	10	2 days	80	4.2	3.6	1.2
5	$SnCl_4$	DCM	5	2 days	RT	4.1	3.4	1.2
6	$SnCl_4$ + $SnCl_4$	DCM	10	2 days	RT	3.1	2.7	1.1
7	Triflic Acid	o-DCB	14	2 days	120	29	15	2.0
8	$AlCl_3$	THF	10	2 days	60	2.8	2.7	1.0

In entries **2**,**4**,**6**, 24 hours after the first addition of 5% $SnCl_4$, a further injection of the same amount of acid was performed. This led to higher polydispersity (entry **2**) and lower molar masses (entry **4**,**6**). In the light of the results, we decided not to add additional Lewis acid in the following tests, with triflic acid and aluminum trichloride.

Analyzing the experimental values, it is clear that the best results were obtained in o-DCB with $SnCl_4$ and with triflic acid.

*Polymerization of **4d** with $SnCl_4$ in o-DCB*

In order to verify the control of the polymerization the increase of molar mass was monitored in function of the monomer conversion. The polymerization of **4d** was performed by $SnCl_4$ (25%), using the solvent (o-DCB) as standard. The collected reaction samples were quenched in water with some drops of hydrazine; the organic layer, withdrawn by syringe, was analyzed by ^1H NMR and GPC (Table 3.2.2).

Table 3.2.2: Experimental result for the polymerization in o-DCB with $SnCl_4$

Sample	***Conversion %***	***M_n [kg/mol]***	***M_w [kg/mol]***	***Đ***
1 min	51.8	2.4	2.5	1.1
5 min	58.8	2.5	2.6	1.1
30 min	60.8	2.8	3.0	1.1
1 h	67.1	3.0	3.2	1.1
2 h	66.7	3.2	3.7	1.1
3 h	71.8	3.4	3.6	1.1
4 h	79.4	3.5	3.8	1.1
5 h	81.7	3.6	4.1	1.1
6 h	74.9	3.8	4.3	1.1
7 h	76.1	3.8	4.7	1.2
8 h	71.1.	3.9	4.7	1.2
9 h	75.3	4.0	5.0	1.2

As clearly displayed in Figure 3.2.1, after 5 hours (80% conversion) there is a linear relation between M_n and conversion, and the dispersity (Đ) remains constant. After that time, the results reported a decrease of conversion, that is physically impossible. To explain these results, it was supposed that the septum closing the flask, had absorbed some solvent in consequence of the high temperature and long reaction time. For this reason, the data collected confirmed the occurrence of controlled polymerization until 5 hours, but after that time it is not possible to have experimental proof of the controlled nature of the mechanism reaction.

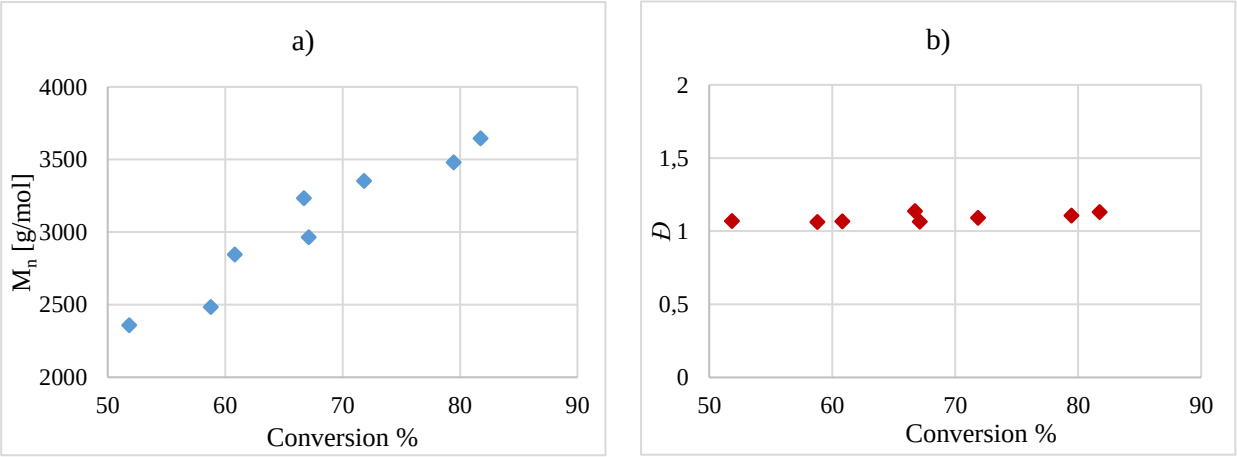

Figure 3.2.1: Relation between a) M_n/conversion; b) Đ/conversion for polymerization with $SnCl_4$ in o-DCB

*Polymerization of **4d** with triflic acid in o-DCB*

The analysis of the polymerization was conducted as above reported for $SnCl_4$. The experimental results are detailed in Table 3.2.3

Table 3.2.3: Experimental result for polymerization in o-DCB with triflic acid

Sample	*Conversion %*	*M_n [kg/mol]*	*M_w [kg/mol]*	*Đ*
1 h	66.4	4.6	2.7	1.7
2 h	69.1	7.9	2.6	2.6
3 h	80.3	5.2	3.0	1.7
4 h	80.2	6.5	3.2	2.0
5 h	77.4	5.8	3.2	1.8
6 h	77.1	8.1	3.3	2.5
7 h	79.1	6.6	3.2	2.1
22 h	85.5	8.0	3.4	2.3
27 h	85.8	6.7	3.4	2.0
31 h	86.1	6.6	3.3	2.0

Analyzing the data of M_n and *Đ* in function of conversion (Figure 3.2.2), is it clear that the polymerization conducted in o-DCB with triflic acid is not controlled.

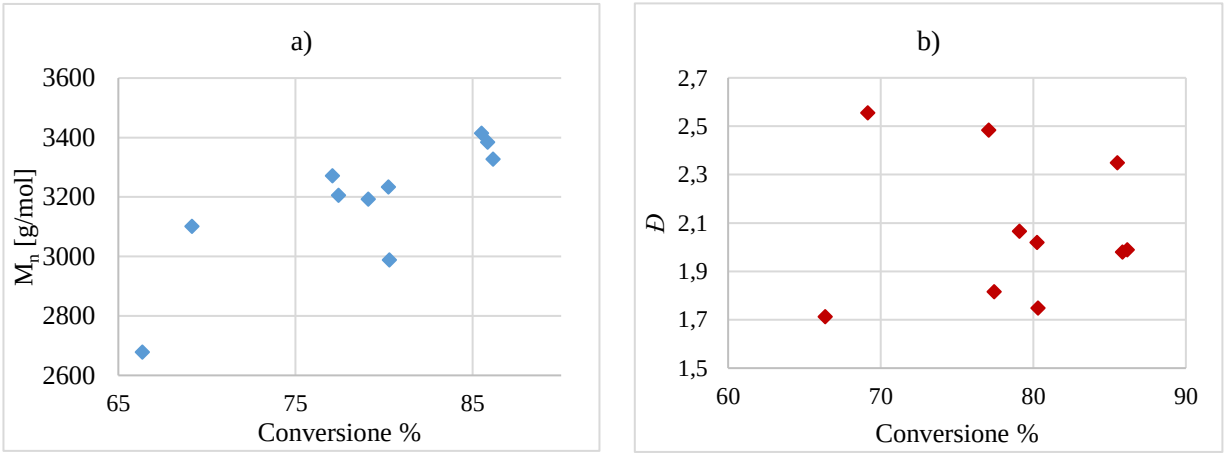

Figure 3.2.2: Relation between a) M_n/Conversion; b) Đ/Conversion for polymerization with triflic acid in o-DCB

3.3 Polymerization with end capping

Thanks to the controlled nature of the polymerization via $SnCl_4$, it is possible to incorporate a functional group at the end of the polymer chain. As end capper we chose a strong nucleophile, *i.e* 4-(*tert*-butyl)phenolate (**10a**) (Scheme 3.3.1).

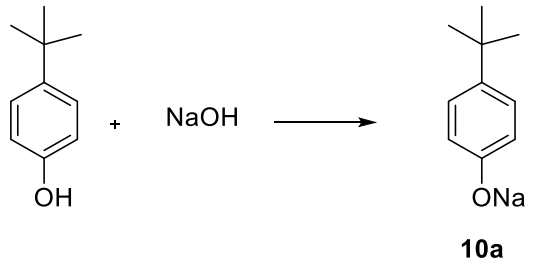

Scheme 3.3.1: Preparation of 10a

The polymerization was conducted using the previously optimized conditions, in o-DCB at 120 °C, adding the end capper to terminate the chains after 24 hours (Scheme 3.3.2). [14]

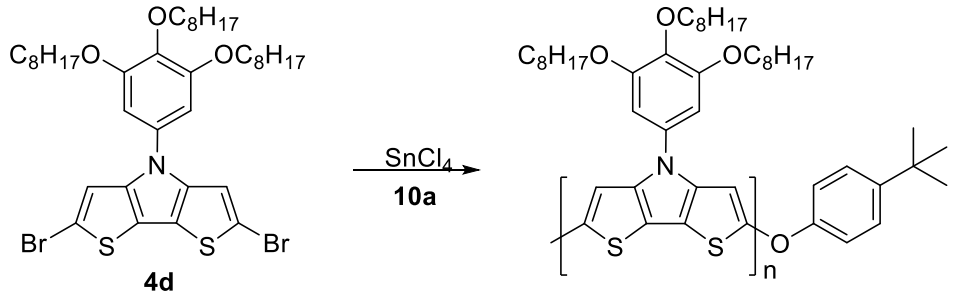

Scheme 3.3.2: Polymerization with end capper (10a)

Unfortunately the ^{1}H NMR signal of the tert-butyl group was overlapped by the signal of the aliphatic chains. For this reason the end capper was changed to one bearing a trimethylsilylgroup, which has a ^{1}H NMR-signal in a less crowded part of the ^{1}H NMR-spectrum (0.1 – 0 ppm). The synthesis of 4-(trimethylsilyl)phenolate (**11b**) followed a procedure reported in literature (Scheme 3.3.3).[15]

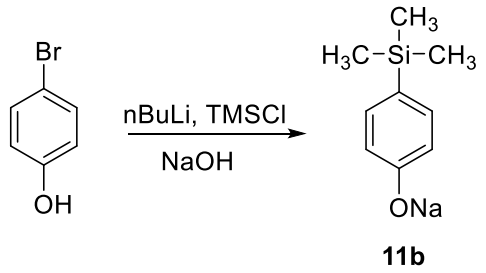

Scheme 3.3.3: Synthesis of 11b

The polymerization was conducted using the same conditions above reported (Scheme 3.3.4).[14]

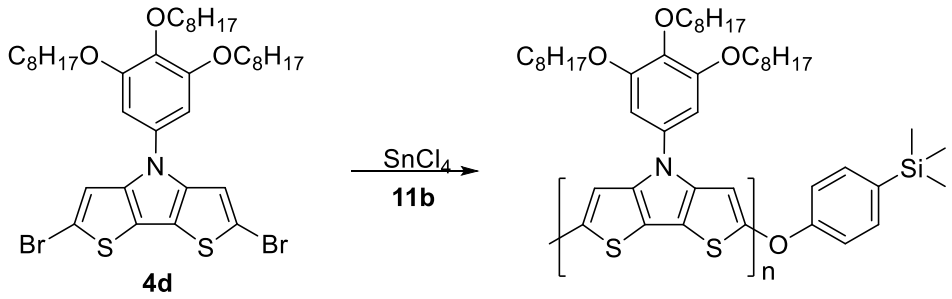

Scheme 3.3.4: Polymerization with end capper (11b)

The polymerization was quenched with methanol and hydrazine, the precipitate was filtered in a Soxhlet thimble and washed with acetone in order to remove the oligomeric fraction and the unreacted monomer. Then, the extraction in chloroform allowed to isolate the polymeric material.

The polymerization was conducted for different times, starting from 5 hours. The recorded data are reported in Table 3.3.1.

Table 3.3.1: Experimental values obtained from controlled polymerization in o-DCB with $SnCl_4$ and end capper (11b)

Time reaction	***Solvent soxhlet extraction***	***Mn [kg/mol]***	***Mw [kg/mol]***	***TMS signal***
5h	Heptane	4.5	6.3	NO
	Chloroform	5.3	8.3	Yes
24 h	Heptane	4.9	7.1	Yes
	Chloroform	6.1	10.6	Yes
48 h	Heptane	8.4	14.5	Yes
	Chloroform	8.8	17.7	Yes

When adding the end capper after 5 hours of reaction, only a small amount of polymeric material with low chain length was formed. Despite this, the ^{1}H NMR of the fraction extracted in chloroform shows an intense signal from the TMS group. That is the experimental evidence of the presence of 4-(trimethylsilyl)phenolate group at the end of the polymer chain. Therefore, even if the polymer was not obtained in a considerable amount, the chains were mostly terminated with **11b**.

In order to increase the chain length, the end capping was performed after 24 hours. The quantity of polymer extracted in chloroform did not increase and the GPC spectrum showed presence of material with high molecular weight also in the fraction extracted in heptane (Figure 3.3.1). These results suggested that the polymer was probably too much soluble in heptane. As reported in Table 3.3.1, the molecular weight increased and the chain would have been enough long to be insoluble in heptane. However after extraction, the amount of polymer was still low (Figure 3.3.1).

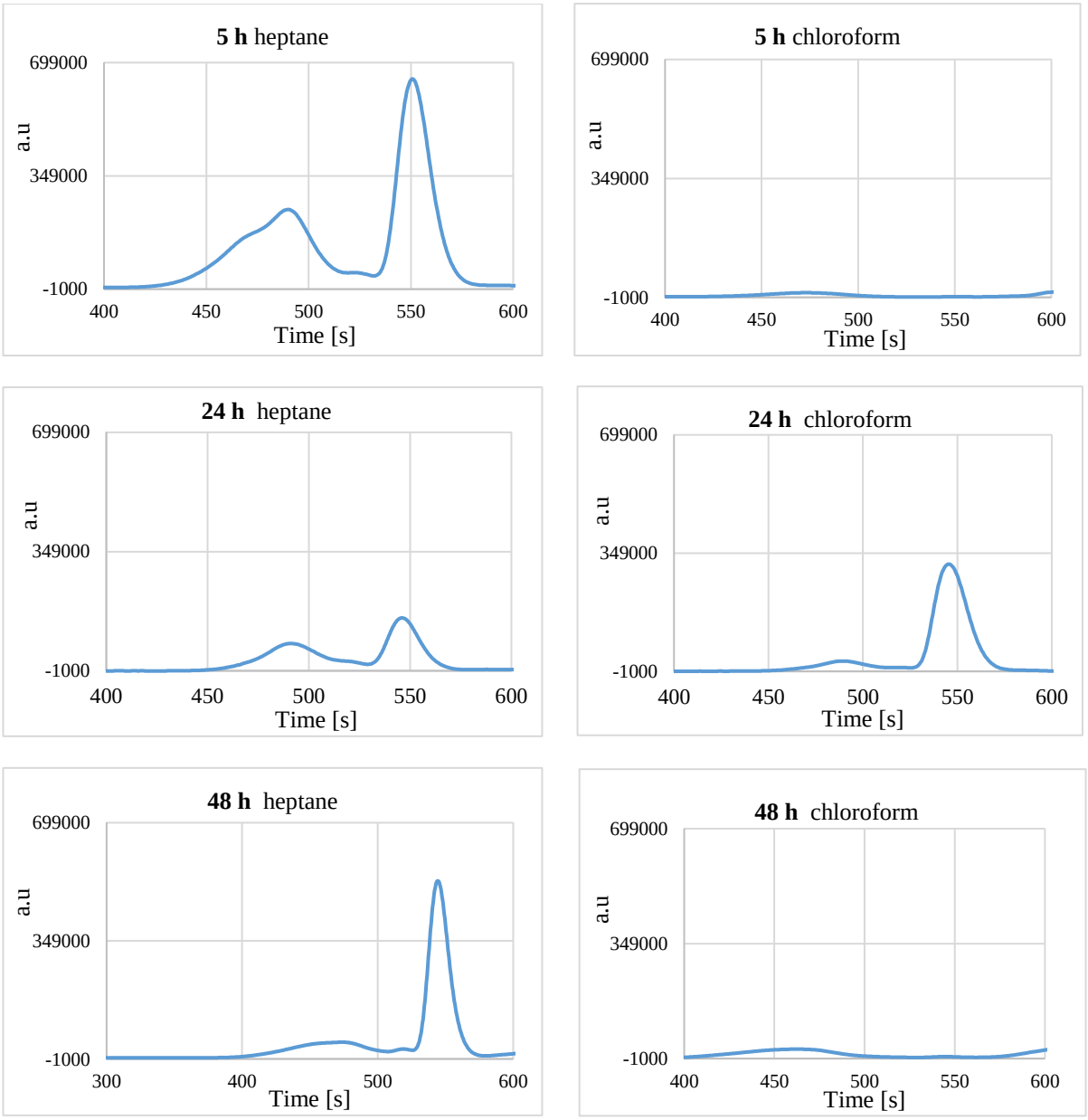

Figure 3.3.1: GPC fraction extracted in heptane and chloroform at different times

A second strategy was to change the solvent used for removing the oligomeric material. The reaction was performed once again, adding **11b** after 72 hours and extracting the oligomers and monomer in acetone, instead of heptane (Table 3.3.2). The GPC spectrum showed absence of polymer in the acetone fraction (Figure 3.3.2) and the ^{1}H NMR reported for the chloroform fraction showed presence of the end capper.

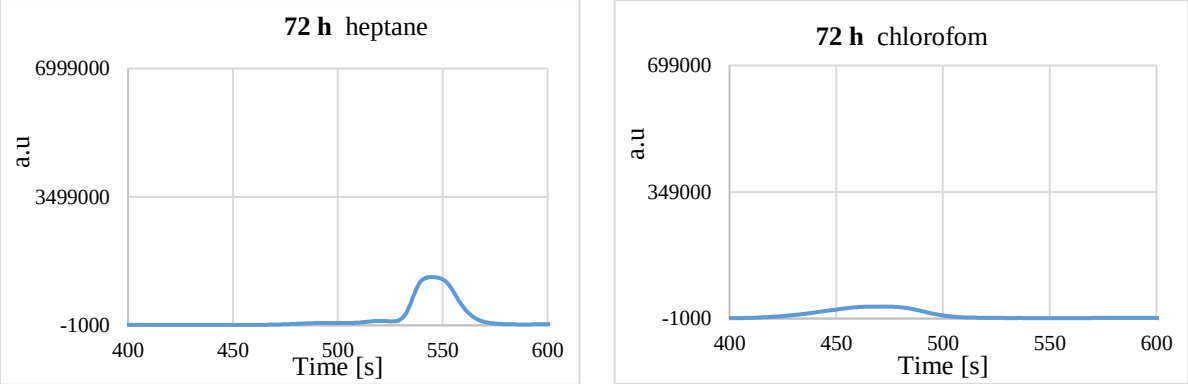

Figure 3.3.2: GPC fraction extracted in heptane and chloroform

Table 3.3.2: Polymerization in o-DCB with $SnCl_4$ and capping after 72 hours

Solvent soxhlet extraction	***M_n [kg/mol]***	***M_w [kg/mol]***
Acetone	3.4	4.9
Chloroform	7.0	10

3.4 Polymerization with chiral derivate

Then, the attention was focused around the behavior of the chiral derivate. In order to investigate "sergeant and soldiers" effect, **5d** was synthetized (Figure 3.4.1).

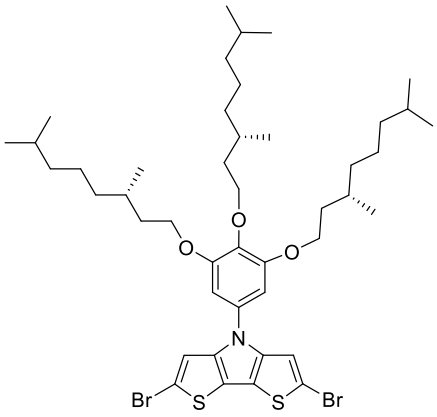

Figure 3.4.1: monomer 5d

The polymerization was done using the procedure previously reported. To different amounts of **5d** and **4d** in o-DCB, 5% of $SnCl_4$ was added. The reaction was stirred for 48 hours at 120 °C. The experimental details are reported in Table 3.4.1

Table 3.4.1: Experimental details

Flask	***5d %***	***5d [mmol]***	***4d %***	***4d [mmol]***	***M_n [kg/mol]***	***M_w[kg/mol]***
Flask 1	0	0	100	0.333	9.4	6.6
Flask 2	20	0.067	80	0.266	13	9.1
Flask 3	40	0.132	60	0.198	17	10
Flask 4	60	0.198	40	0.132	9.0	7.0
Flask 5	100	0.333	0	0	8.8	12

All the reactions were quenched by adding methanol with some drops of hydrazine. The solution was filtered in a Soxhlet thimble and extracted with acetone, in order to remove oligomeric fraction and the unreacted monomer. Then, the extraction in chloroform allowed to isolate the polymeric material. The solid was precipitated in methanol and filtered off. A defined amount of polymer was dissolved in chloroform, adding increasing amounts of methanol. The UV-Vis analysis showed two different bands: at 335 nm the aromatic side chains absorption, while the signal at 525 nm belonged to the polymeric chains. As reported in Figure 3.4.2, the increase of the percent of methanol determines a red shift in UV-Vis, due to aggregation of the macromolecules. However the CD spectra recorded showed the absence of signals for every sample.

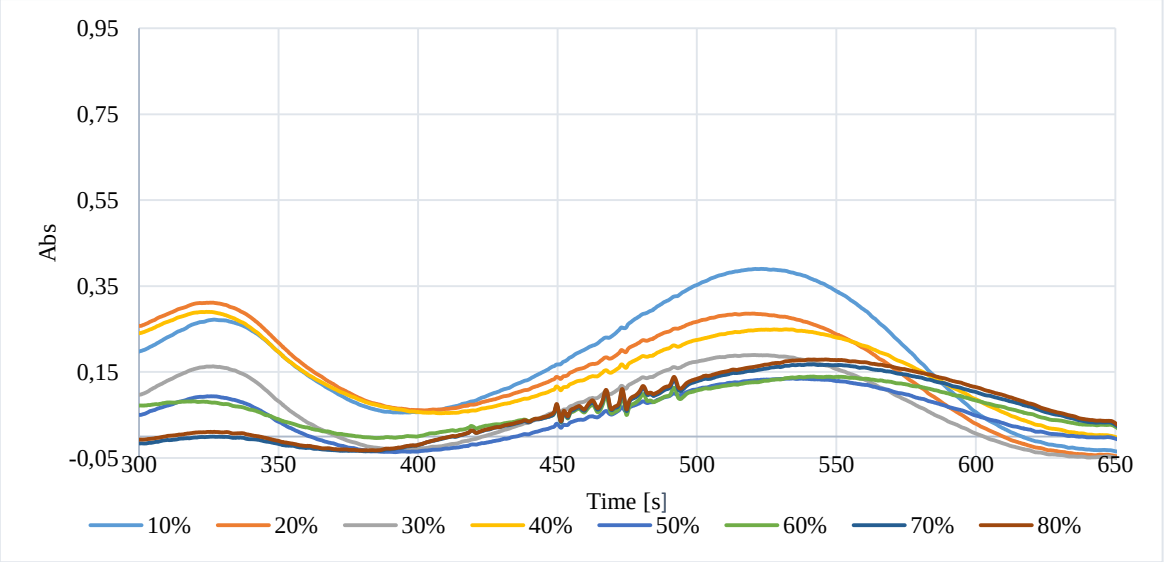

Figure 3.4.2: UV VIS signal of the polymer 100% chiral recorded with solutions with different percent of methanol

In light of what observed, it was supposed that the chains are aggregating but no helical organization can be detected, thus it is impossible to investigate the "sergeants and soldiers" effect. Probably in the polymerization, a mixture of several copolymers is formed with a composition that does not permit the helical organization.

It is necessary to report that the GPC spectra recorded showed a poor amount of polymeric materials, according with the ^{1}H NMR spectrum.

3.5 Copolymerization

Considering the good properties reported in literature of several copolymers, a new experiment was set up to synthetize a block-co-polymer of dithienopyrrole (DTP) and other monomers, polymerized via $SnCl_4$.[16]

The first experiments used a vinyl ether, as the second block of the copolymer (Figure 3.5.1), based on the results by Bonillo and Swager.[14] In order to avoid termination of the active center, the addition of the second monomer was performed at -78 °C. Since o-DCB has a melting point of -17°C, it was necessary to change the solvent. In accordance with the previously obtained results, we conducted the reaction in toluene (Table 3.2.1).

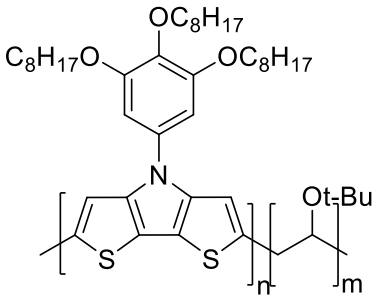

Figure 3.5.1: Block copolymer with vinyl ether

4d was dissolved in dry toluene and $SnCl_4$ was added. After 72 hours at 120 °C, the mixture was cooled down to room temperature and *n*-butyl vinyl ether was added at -78°C. After Soxhlet extraction in acetone and in chloroform, the samples were analyzed by GPC. The chromatograms are here reported (Figure 3.5.2).

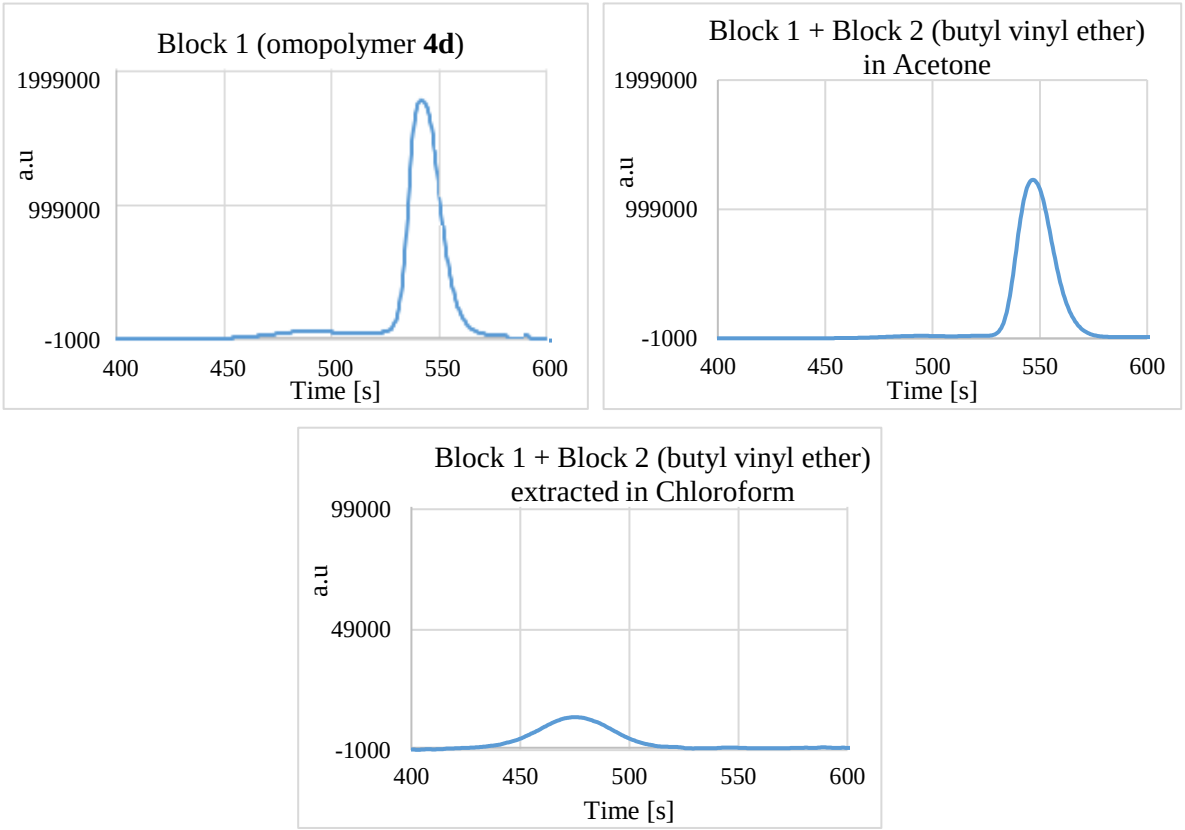

Figure 3.5.2: GPC chromatograms

It is possible to observe that the signal from the polymer did not change after and before the addition of *n*-butyl vinyl ether. The presence of the second block was impossible to check by ^{1}H NMR, because the signals of the *n*-butyl vinyl ether were overlapped by the signal of the first block.

Thus, a different monomer as the alkoxyl derivate **12b** was used. The synthesis is reported in Scheme 3.5.1.

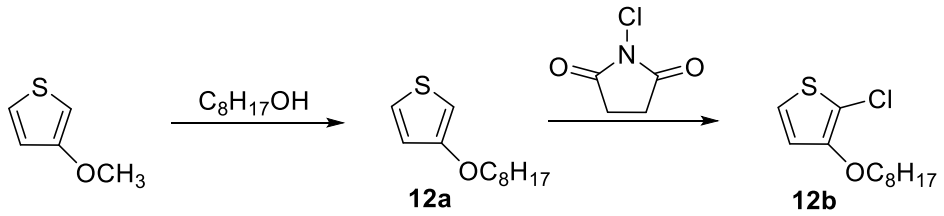

Scheme 3.5.1: Synthesis of 12b

The ^{1}H NMR confirmed the presence of the expected molecule (Figure 3.5.3)

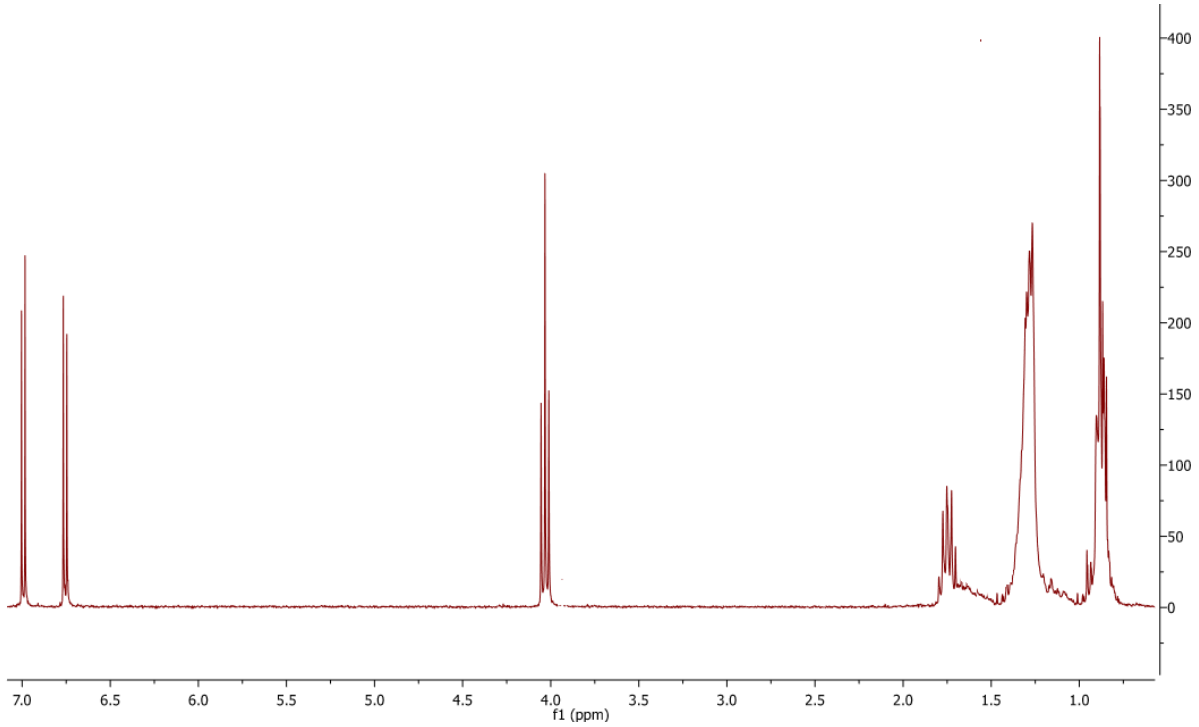

Figure 3.5.3: ^{1}H NMR of 12b

At 6.99 pm and 6.76 pm, the two doublets (1 H each) represent the hydrogens of the aromatic ring. The triplet (4.03 ppm) integrated for 2 protons, is ascribed to the α-hydrogens of the alkyl side-chain. From 1.74 ppm until 0.88 ppm, the signals observed are indistinctly ascribed to the aliphatic chain.

The polymerization of **4d** with **12b** was conducted following a published procedure by Bonillo and Swager.[14] In o-DCB, the monomer of the first block was polymerized with a solution of $SnCl_4$. When the first monomer was used up, the second monomer in o-DCB was added. The experimental results are reported in Table 3.5.1.

Table 3.5.1: Experimental values obtained from copolymerization of 4d with 12b

Copolymer	***Sample***	***Mn [kg/mol]***	***Mw [kg/mol]***
Copolymer 1	*4d*	16	41
	4d + 12b	17	32
Copolymer 2	*12b*	13	19
	12b + 4d	16	34

The *copolymer 1* was synthetized, polymerizing first **4d** than adding **12b**. Differently for the *copolymer 2*, the first monomer reacted was **12b** then the second block was built by **4d.**

Part of the copolymer **4d** – **12b** remained insoluble after Soxhlet extraction in chloroform: for this reason, the M_w decreased after adding the second block (**12b**). Despite this, ^{1}H NMR was measured. The spectrum recorded showed signals of both **4d** and **12b**, confirming the formation of the block copolymer.

In the inverse block copolymer preparation (**12b - 4d**), after the addition of the second block (**4d**) the M_w and M_n increased, as expected.

3.6 Bibliography

1. Miyakoshi, R., Yokoyama, A. & Yokozawa, T. Catalyst-transfer polycondensation. Mechanism of Ni-catalyzed chain-growth polymerization leading to well-defined poly(3-hexylthiophene). *J. Am. Chem. Soc.* **127,** 17542–17547 (2005).

2. Koeckelberghs, G. *et al.* Improved synthesis of N-alkyl substituted dithieno[3,2-b:2′,3′-d]pyrroles. *Tetrahedron* **61,** 687–691 (2005).

3. Han, J., Yin, H., Liu, C., Wang, J. & Jian, X. Construction of donor-acceptor polymers containing thiophene-phthalazinone moiety via classic Ullmann C[sbnd]N coupling polymerization and their optical-electrical properties. *Polym. (United Kingdom)* **101,** 241–256 (2016).

4. Tamba, S., Shono, K., Sugie, A. & Mori, A. C-H functionalization polycondensation of chlorothiophenes in the presence of nickel catalyst with stoichiometric or catalytically generated magnesium amide. *J. Am. Chem. Soc.* **133,** 9700–9703 (2011).

5. Willot, P. & Koeckelberghs, G. Evidence for catalyst association in the catalyst transfer polymerization of thieno[3,2- b]thiophene. *Macromolecules* **47,** 8548–8555 (2014).

6. Yokoyama, A., Miyakoshi, R. & Yokozawa, T. Chain-Growth Polymerization for Poly(3-hexylthiophene) with a Defined Molecular Weight and a Low Polydispersity. *Macromolecules* **37,** 1169–1171 (2004).

7. Valente, C., Belowich, M. E., Hadei, N. & Organ, M. G. Pd-PEPPSI complexes and the Negishi reaction. *European Journal of Organic Chemistry* 4343–4354 (2010). doi:10.1002/ejoc.201000359

8. Valente, C. *et al.* The development of bulky palladium NHC complexes for the most-challenging cross-coupling reactions. *Angew. Chemie - Int. Ed.* **51,** 3314–3332 (2012).

9. Bryan, Z. J., Smith, M. L. & McNeil, A. J. Chain-growth polymerization of aryl grignards initiated by a stabilized NHC-Pd precatalyst. *Macromol. Rapid Commun.* **33,** 842–847 (2012).

10. Lanni, E. L., Mcneil, A. J., Uni, N., V, V. a & Arbor, A. Mechanistic Studies on Ni(dppe) Cl2 -Catalyzed Chain-Growth Polymerizations : Evidence for Rate-Determining Reductive Elimination. *J. Am. Chem. Soc.* **131,** 16573–16579 (2009).

11. Barron, A. R. P-31 NMR Spectroscopy 1 Introduction 3 Interpreting spectra. 1–11 (2013).

12. Sheina, E. E., Liu, J., Iovu, M. C., Laird, D. W. & McCullough, R. D. Chain growth mechanism for the regioregular nickel inititated cross-coupling polymerisations. *Macromolecules* **37,** 3526–3528 (2004).

13. Bronstein, H. A. & Luscombe, C. K. Externally initiated regioregular P3HT with controlled molecular weight and narrow polydispersity. *J. Am. Chem. Soc.* **131,** 12894–12895 (2009).

14. Bonillo, B. & Swager, T. M. Chain-growth polymerization of 2-chlorothiophenes promoted by lewis acids. *J. Am. Chem. Soc.* **134,** 18916–18919 (2012).

15. Brenzovich, Jr., W., Brazeau, J.-F. & Toste, F. Gold-Catalyzed Oxidative Coupling Reactions. *Org. Lett.* **12,** 4728–4731 (2010).

16. Rasmussen, S. C. & Evenson S. J. Dithieno[3,2-b:2′,3′-d]pyrrole-based materials Synthesis and application to organic electronics. *Prog. Polym. Sci.* **38,** (2013).

CHAPTER 4: CONCLUSION

The aim of the presented project was to verify the possibility to perform a controlled polymerization and then using that polymerization to prepare a series of achiral and chiral monomers for verifying the "sergeants and soldiers" effect.

This project started by investigating the possibility to obtain a controlled polymerization of PDTP. Monomers with different side chains and organometallic functions were screened for a CTCP-type polymerization. First attempt, **2d** was synthetized and polymerized with $Ni(dppp)Cl_2$. GPC clearly showed that the main products present after the polymerization were dimer/trimer and monomer. In order to decrease the unstable nature of the monomer, due to the electron rich character of the system, a new derivate, **4c**, was synthetized. The polymerization was performed via KCTCP, tuning the ligand of Ni based catalysts. The poor results obtained led us to change the catalytic center, using a Pd based catalyst. The GPC analysis revealed the same result obtained as for the Ni – catalysts. Since it was confirmed that the problem was not due to the nature of metal or of ligand, we therefore focused on the mechanism of reaction. A test reaction and ^{31}P NMR analysis revealed that during the OA the catalyst was unable to insert because of the electron rich nature of the monomer.

It was decided to change the method of polymerization to a cationic polymerization, using Lewis acids. Different conditions were screened, and the best results were obtained in o-DCB at 120 °C, with triflic acid and with $SnCl_4$. Checking the polymerization, only the reaction in $SnCl_4$ was controlled. An additional proof of the controlled nature of the polymerization was obtained by end-capping the polymer after polymerization.

Then, the attention was focused around the behavior of the chiral derivate. In order to investigate the "sergeants and soldiers" effect, a chiral derivate **5d** was synthetized and polymerized with different amounts of achiral DTP, **4d**. However, no CD-signal could be observed. In this condition the presence of "sergeants and soldiers" effect was impossible to verify.

Because of the controlled nature of the polymerization, it was possible to synthesize block copolymers. The block copolymer **4d-12b** was poorly soluble, and the physical

characterization was difficult. Despite this, the GPC signal confirmed the formation of the block polymer. Block copolymer **12b-4d** was soluble: the characterization showed that the polymer had a high molar mass, but also the dispersity was high.

In conclusion, the presented research project showed that a controlled polymerization and a consequent controlled end capping for PDTP is possible. It is also proven that block copolymers of different electron rich monomers could be synthesized. Several combination of monomers could be polymerized in order to improve the physical and chemical properties. Moreover, despite the absence of a CD signal with **5d**, exploring the behavior of the polymer of chiral PDTP remains interesting.

CHAPTER 5: EXPERIMENTAL PART

5.1 Synthesis of 2-bromo-4-dodecyl-dithieno[3,2-*b*:2',3'-*d*]pyrrole (2b)

Step 1: Synthesis of 4-dodecyl-dithieno[3,2-*b*:2',3'-*d*]pyrrole **(2a)**

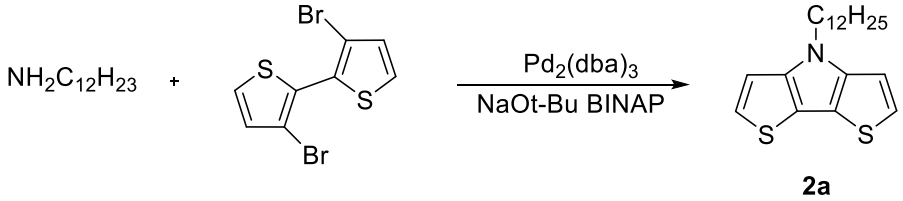

2a

A solution of 3,3'-dibromo-2,2'–bithiophene (5.30 g, 16.4 mmol), BINAP (1.02 g, 1.64 mmol), $Pd_2(dba)_3$ (0.374 g, 0.409 mmol) and NaO*t*-Bu (3.79 g, 39.3 mmol) in dry toluene, was purged with N_2. Dodecyl amine (3.05 g, 16.4 mmol) was added. The solution was stirred for 7 hours at 110°C and checked by TLC (SiO_2, heptane/DCM, 90/10). The flask was cooled down and water was added. The water layer was extracted with DCM. The organic layer was dried with $MgSO_4$. The solvent was removed under vacuum and the crude product was purified by column chromatography (heptane/DCM, 80/20). The product was isolated as a transparent oil (3.65 g, 64 %).

^{1}H-NMR ($CDCl_3$, 300MHz, ppm): δ 7.13 (d, J = 5.3 Hz, 2H); 7.00 (d, J = 5.3 Hz, 2H); 4.19 (t, 2H); 1.80-1.24 (m, 20H); 0.88 (t, 3H).

Step 2: Synthesis of 2-bromo-4-dodecyl-dithieno[3,2-*b*:2',3'-*d*]pyrrole **(2b)**

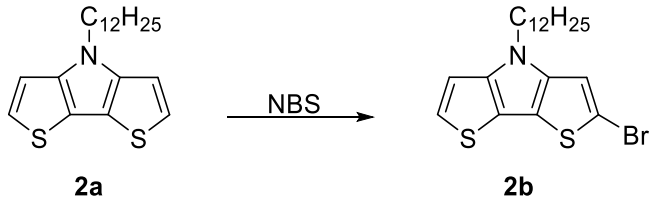

2a **2b**

NBS (0.854 g, 4.80 mmol) in 40 ml of THF was added to a stirred solution of 4-dodecyl-dithieno[3,2-*b*:2',3'-*d*]pyrrole (3.65 g, 10.5 mmol) in THF at 0°C. The mixture was stirred at this temperature for 1 hour. The reaction was monitored via TLC (SiO_2, heptane/DCM, 80/20). After complete conversion, an aqueous solution of $Na_2S_2O_3$ was added and the product was extracted with Et_2O. The organic layer was washed with $NaHCO_3$ and dried using $MgSO_4$. After filtration, the solvent was removed by rotary evaporation. The crude product was purified by column chromatography (SiO_2, heptane/DCM, 80/20) and the product was obtained as yellow viscous oil (0.591 g, 0.865 mmol) (7.6%).

^{1}H-NMR ($CDCl_3$, 300MHz, ppm): δ 7.13 (d, *J* = 5.3 Hz, 1H); 7.05 (s, 1H); 6.98 (d, *J* = 5.3 Hz, 1H); 4.12 (t, 2H); 1.80-1.24 (m, 20H); 0.88 (t, 3H).

5.2 Polymerization of 2b via Kochel Houser base

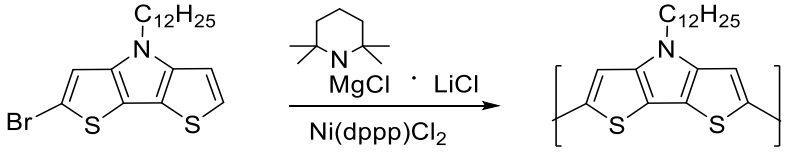

2b

A flask with 1 ml of TMPMgCl · LiCl (1.00 mmol) was cooled down to – 78 °C and the solution was purged with nitrogen. The content was transferred to a flask, previously cooled

down and purged, with **2b** (1.41 mmol , 0.426 g). The resulting mixture was stirred at -78 °C until complete dissolution of **2b**.

The monomer was then added to Ni(dppp)Cl_2 (3.90 mg, 0.00704 mmol) in dry THF.

GPC Ni(dppp)Cl_2: M_w 1.8 kg/mol, M_n 1.1 kg/mol.

5.3 Synthesis of 3,4,5-tri(octyloxy)aniline (3c)

Step 1: Synthesis 1,2,3-tri(octyloxy)benzene **(3a)**

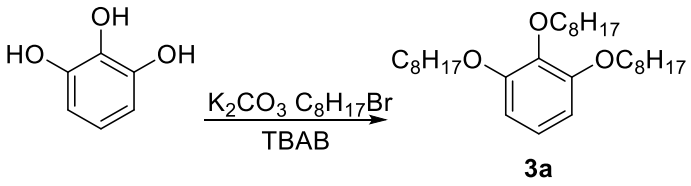

3a

A solution of benzene-1,2,3-triol (6.34 g, 50.3 mmol), K_2CO_3 (41.4 g, 300 mmol), 1-bromooctane (28.5 ml, 162 mmol), tetra-butylammonium bromide (0.808 g, 2.51 mmol) in 250 ml of MIBK was added to a flask. The solution was refluxed for 5 hours. The reaction was monitored by TLC (SiO_2, DCM/heptane, 20/80). Once the reaction was completed, the solution was cooled to room temperature and 300 ml of water was added. The product was then extracted with DCM. The organic layer was washed with HCl and $NaHCO_3$ and dried with $MgSO_4$. After filtration, the solvent was evaporated by rotary evaporation. The crude product was purified by column chromatographic (50/50, heptane/DCM). The product was isolated as oil with yield of 94 %.

^{1}H-NMR ($CDCl_3$, 300 MHz, ppm): δ 6.91 (t, *J* = 8.3 Hz 1H); 6.54 (d, *J* = 8.3 Hz 2H); 3.95 (dd, 6H); 1.83-1.07 (m, 36H); 0.87 (t, 9H).

Step 2: Synthesis of 5-nitro-1,2,3-tri(octyloxy)benzene **(3b)**

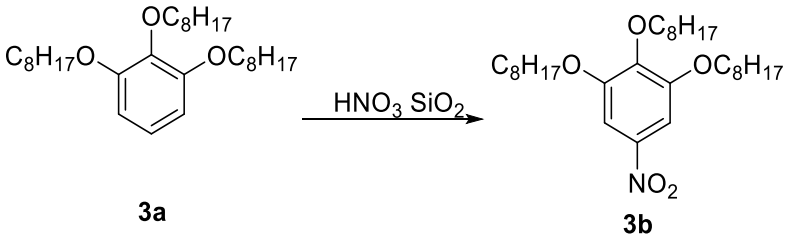

3a **3b**

SiO_2 (65.9 g, 3.96 mmol) was suspended in DCM (150 ml). HNO_3 (3.92 ml, 5.54 mmol) was added. The resulting suspension was stirred for 10 minutes at RT. **3a** (20.3 g, 47.5 mmol) was dissolved in DCM and added. The suspension was stirred for 2 hour. After reaction, $NaHCO_3$ was added until gas evolution ceased. The solution was filtered and the solvent was evaporated by rotary evaporation. The resulting product was dissolved in a small amount of o-DCB and precipitated in 500 ml of ice cooled MeOH. The resulting solution was filtered and washed with MeOH. After drying under vacuum, a yellow solid was obtained (59 %).

^{1}H-NMR ($CDCl_3$, 300 MHz, ppm): δ 7.26 (s, 2H); 4.04 (dd, 6H); 1.83-1.07 (m, 36H); 0.87 (t, 9H).

Step 3: Synthesis of 3,4,5-tri(octyloxy)aniline **(3c)**

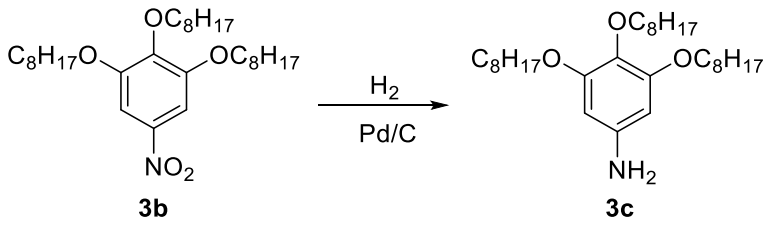

3b **3c**

A solution of **3b** (14.2 g, 27.9 mmol) in 100 mL of 50/50 EtOH/EtOAc, was purged with cycle N_2/Vacuum. 0.05 equivalent of Pd/C (0.148 g, 1.39 mmol) were added. The flow of N_2 was changed to a flow of H_2. The solution was stirred for 24 hours at room temperature. After filtration, the solvent was evaporated by rotary evaporation. The product was obtained as a transparent oil (12.2 g, 25.5 mmol). (yield = 91 %)

^{1}H-NMR ($CDCl_3$, 300 MHz, ppm): δ 5.91 (s, 2H); 5.30 (s, 2H); 3.89 (dd, 6H); 1.28-1.80 (m, 36H); 0.89 (m, 9H);

5.4 Synthesis of 2-bromo-6-iodo-4-(3,4,5-tri(octyloxy)phenyl)dithieno[3,2-*b*:2',3'-*d*]pyrrole (4c)

Step 1: Synthesis of 4-(3,4,5-tri(octyloxy)phenyl)dithieno[3,2-*b*:2',3'-*d*]pyrrole **(4a)**

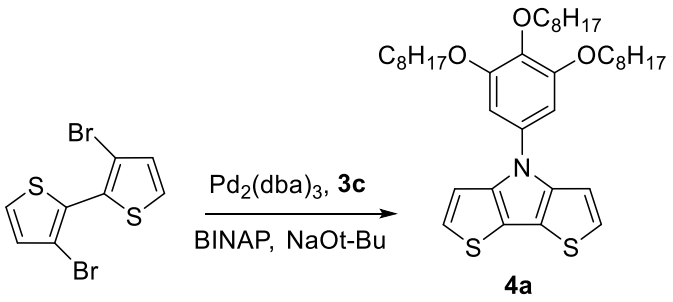

A solution of 3,3'-dibromo-2,2'–bithiophene (4.26 g, 13.1 mmol), BINAP (0.806 g, 1.31 mmol), NaO*t*-bu (3.04, 31.5 mmol), $Pd_2(dba)_3$ (0.300 g, 0.328 mmol) in dry toluene, was purged with N_2. **3c** was added (6.28 g, 13.1 mmol). The solution was stirred for 8 hours at 110°C and checked by TLC (SiO_2, heptane/DCM, 90/10). Once cooled down, water was added. The water layer was extracted with diethyl ether and the organic layer was dried with $MgSO_4$. The crude compound was purified by column chromatography (SiO_2, heptane/DCM, 80/20), in order to obtain the pure product (6.79 g, 8.52 mmol), as pale oil (65 %).

^{1}H-NMR ($CDCl_3$, 300 MHz, ppm): δ 7.16 (q, *J* = 5.3 Hz, 4H); 6.74 (s, 2H); 4.00 (dd, 6H); 1.81- 1.30 (m, 36H); 0.88 (m, 9H).

Step 2: Synthesis of 2-bromo-4-(3,4,5-tris(octyloxy)phenyl)-dithieno[3,2-*b*:2',3'-*d*]pyrrole **(4b)**

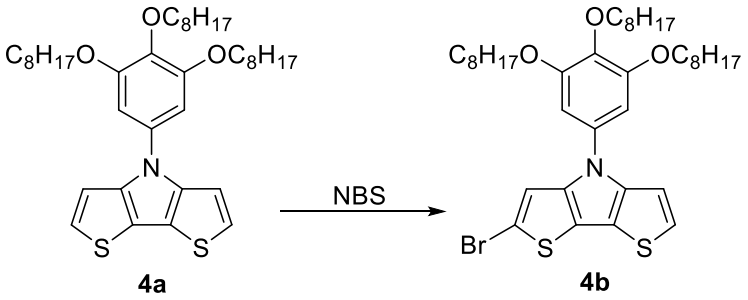

One equivalent of NBS (0.782 g, 4.39 mmol) was added to a solution of **4a** (2.79 g, 4.36 mmol) in THF at 0°C. The mixture was stirred at RT for 2 hours. After complete of reaction (TLC-monitoring, SiO_2, heptane/DCM, 80/20), the solution was washed with $NaHCO_3$ and $Na_2S_2O_3$. Then, the solution was extracted twice with diethylether. The organic layer were combined and dried with $MgSO_4$. After filtration, the solvent was removed by rotary evaporation. The crude product was purified by column chromatography (SiO_2, heptane/DCM, 80/20) in order to obtain a brown viscous oil (0.591 g, 0.865 mmol) (20 %).

^{1}H-NMR ($CDCl_3$, 300MHz, ppm): δ 7.18 (m, 2H); 7.11 (m, 1H); 6.68 (s, 2H); 4.00 (dd, 6H); 1.28-1.80 (m, 36H); 0.87 (m, 9H).

Step 3: Synthesis of 2-bromo-6-iodo-4-(3,4,5-tri(octyloxy)phenyl)dithieno[3,2-*b*:2',3'-*d*]pyrrole **(4c)**

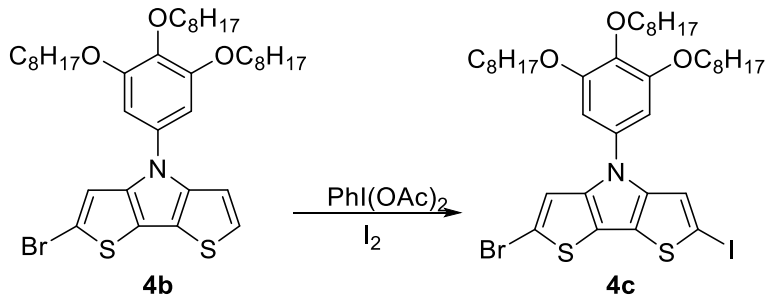

Iodine (0.591 g, 0.865 mmol) and iodobenzene diacetate (0.136 g, 0.517 mmol) were added to a stirred solution of **4b** (0.591 g, 0.865 mmol) in DCM at 0 °C. The mixture was stirred at room temperature for 4 h, the reaction was monitored with TLC (SiO_2, heptane/DCM, 80/20). An aqueous solution of $Na_2S_2O_3$ was added, and the mixture was extracted with DCM. The organic layer was dried with $MgSO_4$. After filtration, the solvent was removed by rotary evaporation. The crude product was purified by high vacuum, in order to obtain a brown viscous oil (0.427 g, 0.506 mmol) (12%).

^{1}H-NMR ($CDCl_3$, 300MHz, ppm): δ 7.12 (s, 1H); 6.62 (s, 2H); 3.99 (dd, 6H); 1.28-1.80 (m, 36H); 0.89 (m, 9H).

5.5 Synthesis of 2,6-dibromo-4-(3,4,5-tri(octyloxy)phenyl) dithieno[3,2-*b*:2',3'-*d*]pyrrole (4d)

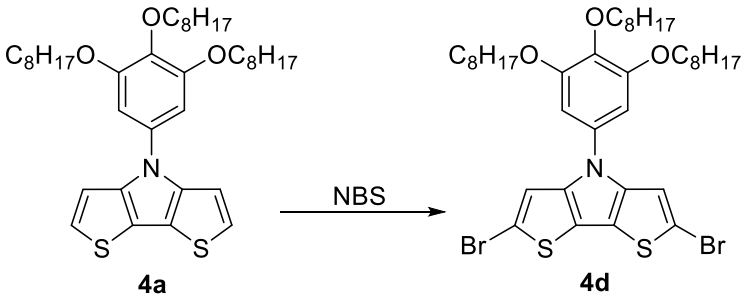

4a **4d**

NBS (5.11 g, 28.7 mmol) was added to a solution of **4a** (9.18 g, 14.4 mmol) in THF at 0°C. The mixture was stirred at RT overnight. After complete of reaction (TLC-monitoring, SiO_2, heptane/DCM, 80/20), the solution was washed with $NaHCO_3$ and $Na_2S_2O_3$. Then, the solution was extracted twice with diethylether. The organic layers were combined and dried with $MgSO_4$. After filtration, the solvent was removed by rotary evaporation. The crude product was purified by column chromatography (SiO_2, heptane/DCM, 80/20) in order to obtain a brown viscous oil (0.591 g, 0.865 mmol) (86 %).

^{1}H-NMR ($CDCl_3$, 300MHz, ppm): δ 7.09 (s, 2H); 6.62 (s, 2H); 3.99 (q, 6H); 1.95-1.28 (m, 36H); 0.88 (m, 9H).

5.6 Synthesis of 2,6-dibromo-4-(3,4,5-tri((3,7-dimethyloctyl)oxy)phenyl)dithieno[3,2-b:2',3'-d]pyrrole (5d)

Step 1: Synthesis of 4-(3,4,5-tri((2,7-dimethyloctyl)oxy)phenyl)dithieno[3,2-*b*:2',3'-*d*]pyrrole **(5a)**

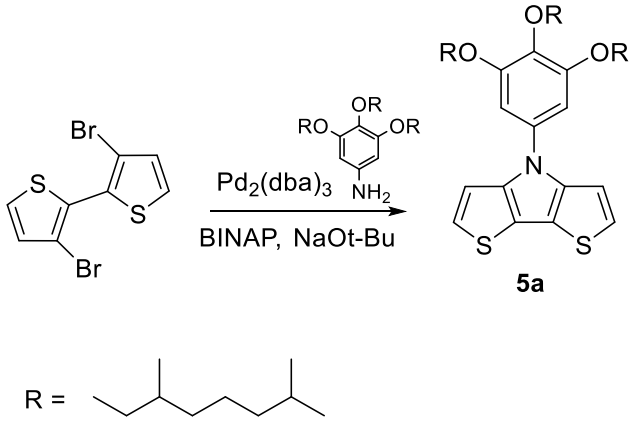

A solution of 3,3'-dibromo-2,2'–bithiophene (0.773 g, 2.38 mmol), BINAP (0.148 g, 0.238 mmol), NaO*t*-Bu (0.550, 5.72 mmol), $Pd_2(dba)_3$ (0.00596 g, 0.00546 mmol) in dry toluene, was purged with N_2. 3,4,5-tri((2,7-dimethyloctyl)oxy)aniline was added (1.34 g, 1.34 mmol). The solution was stirred for 8 hours at 110°C and checked by TLC (SiO_2, heptane/DCM, 90/10). Once cooled down, water was added. The water layer was extracted with diethyl ether and the organic layer was dried with $MgSO_4$. The crude compound was purified by column chromatography (SiO_2, heptane/DCM, 50/50), in order to obtain the pure product (6.79 g, 8.52 mmol), as pale oil (65 %).

^{1}H-NMR ($CDCl_3$, 300 MHz, ppm): δ 7.16 (q, J = 5.3 Hz, 4H); 6.74 (s, 2H); 4.00 (q, 6H); 1.95-1.07 (m, 39H); 0.87 (m, 18H).

Step 2: Synthesis of 2,6-dibromo-4-(3,4,5-tri((3,7-dimethyloctyl)oxy)phenyl)dithieno[3,2-*b*:2',3'-*d*]pyrrole **(5d)**

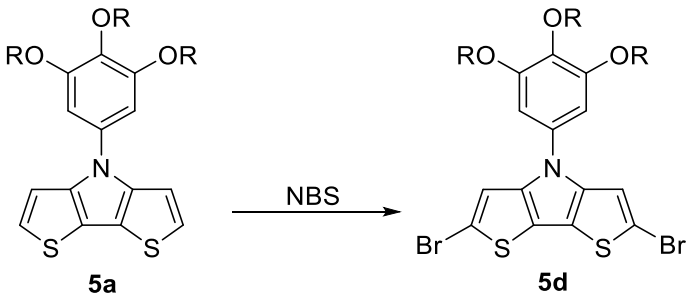

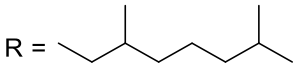

NBS (0.295 g, 1.66 mmol) was added to a solution of **5a** (0.563 g, 0.830 mmol) in THF at 0°C. The mixture was stirred at RT overnight. After complete of reaction (TLC-monitoring, SiO_2, heptane/DCM, 80/20), the solution was washed with $NaHCO_3$ and $Na_2S_2O_3$. Then, the solution was extracted twice with diethylether. The organic layers were combined and dried with $MgSO_4$. After filtration, the solvent was removed by rotary evaporation. The crude product was purified by column chromatography (SiO_2, heptane/DCM, 80/20) in order to obtain a brown viscous oil (0.530 g, 0.634 mmol) (76 %).

^{1}H-NMR ($CDCl_3$, 300MHz, ppm): δ 7.13 (s, 2H); 6.62 (s, 2H); 3.99 (q, 6H); 1.95-1.28 (m, 39H); 0.88 (m, 18H).

5.7 Polymerization via Kumada Method of 4c

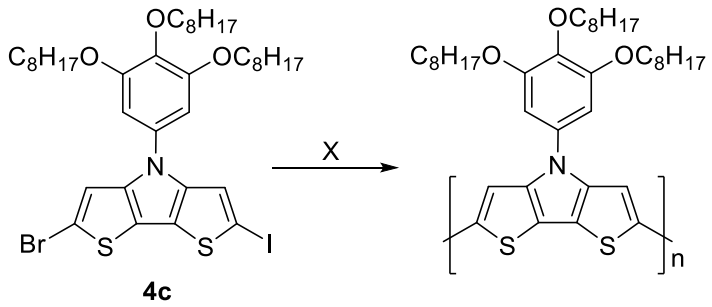

4c

X = $Ni(dppp)Cl_2$
$Ni(NHC)Cl_2$
$Ni(dppe)Cl_2$
PEPPSI Pd

All glassware was ovendried for one night and purged with N_2.

4c (0.730 ml, 0.825 mmol) in dry THF was dissolved; *i*-PrMgCl·LiCl (0.77 ml, 0.825 mmol) was added in a tube. The solution was made up until 8.25 ml with dry toluene and was stirred in ice bath.

In four different flasks, the catalyst were dissolved 1 ml of dry THF (Table 5.7.1).

Table 5.7.1: Details of the solution prepared

Flask	***Catalyst***	***mmol***	***g***
Flask 1	$Ni(dppp)Cl_2$	0.01	0.0053 g
Flask 2	$Ni(NHC)Cl_2$	0.01	0.0074 g
Flask 3	$Ni(dppe)Cl_2$	0.01	0.0055 g
Flask 4	PEPPSI Pd	0.01	0.0070 g

2 ml of the solution previously prepared, was added in *Flask 1*, *Flask 2*, *Flask 3*. In order to polymerize using PEPPSI Pd, it was necessary to use a different organometallic derivate of

the monomer (Zn derivate). For this reason, a solution of $ZnBr_2$ (0.0564 g, 0.240 mmol) in THF was prepared. This solution was added to *Flask 4* and the monomer was added.

The mixture is stirred at RT for a 30 minutes. The content of the four flask is checked by GPC (Table 5.7.2).

Table 5.7.2: Details of experimental analysis

Flask	*Catalyst*	M_w *[kg/mol]*	M_n *[kg/mol]*
Flask 1	$Ni(dppp)Cl_2$	2.8	2.5
Flask 2	Ni(NHC)	1.2	0.95
Flask 3	$Ni(dppe)Cl_2$	2.7	2.4
Flask 4	PEPPSI Pd	1.5	1.2

5.8 Polymerization via KCTCP (^{31}P analysis) of 4c

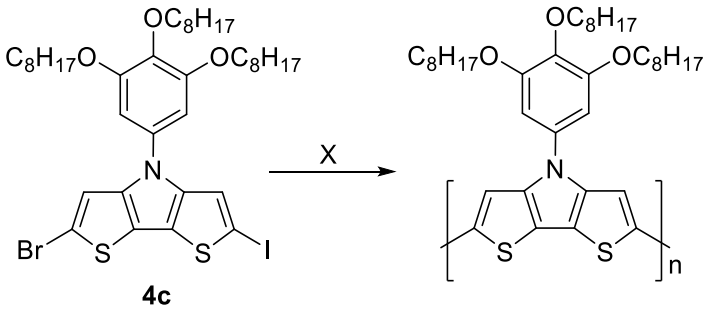

4c

X = $Ni(dppp)Cl_2$
o-tolyl- $Ni(dppp)Cl_2$

All the glassware was ovendried for one night and purged with N_2.

0.9 equivalents of *i*-PrMgCl · LiCl (0.148 ml, 0.200 mmol) were added to 0.642 ml of 2-bromo-6-iodo-4-(3,4,5-tri(octyloxy)pheny)dithieno[3,2-*b*:2',3'-*d*]pyrrole in dry THF. The solution was stirred in an ice bath, 0.246 ml (0.100 mmol) was added to an NMR tube previously prepared with 0.3 ml of dry THF and one of the two catalyst.

Catalyst 1: 10.8 mg (0.02 mmol) of Ni(dppp)Cl_2, was added in a flask with 0.3 ml of dry THF.

Catalyst 2: a solution of 16.5 mg (0.04 mmol) of 1,3-bis(diphenylphosphino)propane and 17.2 mg of o-tolyl-Ni(dppp)Cl_2, (0.02 mmol) in 0.3 ml of dry THF was prepared.

^{31}P NMR (THF, H_3PO_4, ppm) o-tolyl: δ 27.12 (s); 20.90 (d); -4.38 (d); -5.16 (s); -17.39 (s).

^{31}P NMR (THF, H_3PO_4, ppm) (1,3-dppp)$NiCl_2$: Catalyst is not soluble. No signal.

^{31}P NMR (THF, H_3PO_4, ppm) o-tolyl + Grignard: δ 11.99 (s); - 5.24 (s); -17.39 (s).

^{31}P NMR (THF, H_3PO_4, ppm) (1,3-dppp)$NiCl_2$ + Grignard: Catalyst is not soluble. No signal.

GPC analysis Grignard: M_w 0.82 kg/mol; M_n 0.55 kg/mol

GPC analysis Ni(dppp)Cl_2: M_w 1.5 kg/mol; M_n 0.65 kg/mol

GPC analysis o-tolyl-Ni(dppp)Cl_2: M_w 0.95 kg/mol; M_n 0.39 kg/mol

5.9 Test reaction with 6a

Step 1: 2,5-dibromo-3-hexylthiophene **(6a)**

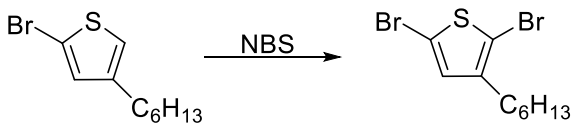

6a

A solution of 2-bromo-4-hexylthiophene (0,00226 mmol, 0.560 g) in THF is stirred in a flask. Then, a solution of 0.871 g (0.00485 mmol) of NBS in THF was added dropwise. The mixture was stirred at RT for 48 hours. The reaction was checked via TLC (SiO_2, heptane). After addition of a solution of $Na_2S_2O_3$, the mixture was extracted with Et_2O. The organic layer was washed successively with $NaHCO_3$, and dried over anhydrous $MgSO_4$. The solvent was removed by rotary evaporation and the product was purify by column chromatographic (SiO_2, heptane). The product was obtained as an oil (85%).

^{1}H-NMR ($CDCl_3$, 300MHz, ppm): δ 6.78 (s, 1H); 2.50 (m, 2H); 1.61-1.32 (m, 8H); 0.89 (t, 3H).

Step 2a: 2,5-diphenyl-3-hexylthiophene **(7a/7b)**

*Confirm absence of reaction between **6a** and phenylmagnesium chloride*

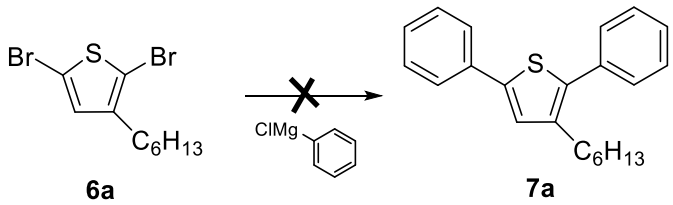

6a **7a**

6a (0.186 g, 0.567 mmol) was added to an oven-dried flask with a solution of phenylmagnesium chloride in THF (2 ml, 2.00 mmol). The reaction was quenched with water, and Et_2O was added. The organic layer was isolated and the solvent was removed by rotary evaporation. The product was analyzed via GC/MS.

*Synthesis of **7a***

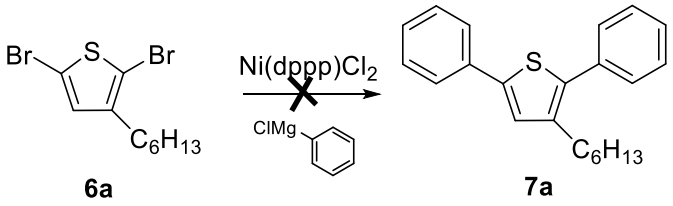

6a **7a**

6a (0.186 g, 0.567 mmol) was added to an oven-dried flask with a solution phenylmagnesium chloride in THF (2 ml, 2 mmol). The mixture was stirred at 0°C, then was added to a solution of $Ni(dppp)Cl_2$ in THF (0.0013 g, 0.0024 mmol). The solution was stirred for 1 hour at 0 °C. The reaction was quenched by adding HCl in THF. The product was analyzed via GC/MS.

Step 2.b: 2,5-di(2-thienyl)-3-hexylthiophene **7c**

*Confirm absence of reaction between **6a** and thiophen-2-ylmagnesium chloride*

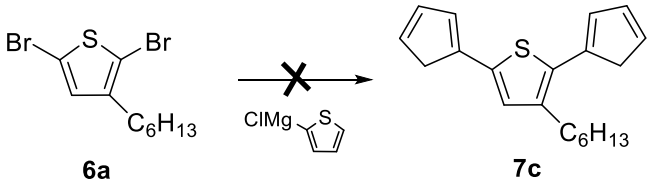

6a **7c**

6a (0.186 g, 0.567 mmol) was added in an oven-dried flask, with a solution of thiophen-2-ylmagnesium chloride in THF (0.567 ml, 0.567 mmol). The reaction was quenched with water, and Et_2O was adding. The organic layer was isolated and the solvent was removed by rotary evaporation. The product was analyzed via GC/MS.

*Synthesis of **7c***

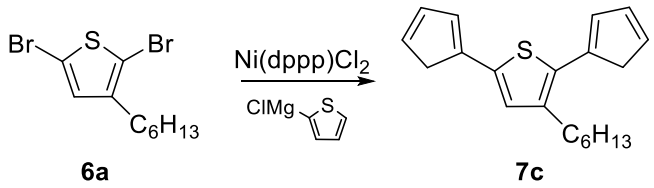

6a **7c**

To an oven-dried flask was added **6a** (0.186 g, 0.567 mmol) and Ni(dppp)Cl_2 (0.0015 g, 0.0028 mmol). The mixture was stirred at 0°C, then a solution of thiophen-2-ylmagnesium chloride in THF (0.567 ml, 0.567 mmol) was added. The solution was stirred for 12 hour at RT. The reaction was quenched with water. The product was analyzed via GC/MS.

5.10 Test reaction with 4d

*Confirm absence of reaction between **4d** and thiophen-2-ylmagnesium chloride*

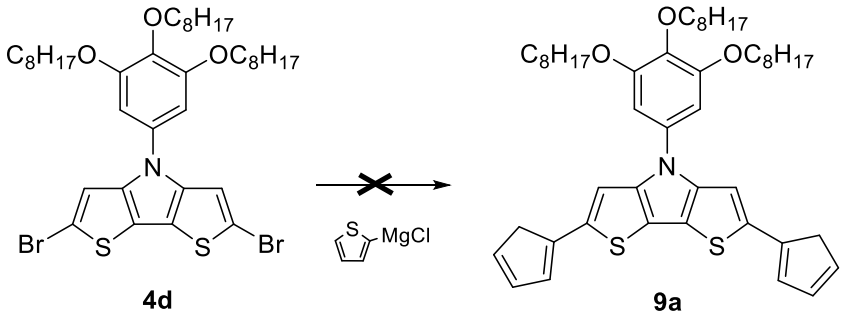

4d **9a**

4d (0.543 g, 0.567 mmol) was added to an oven-dried flask with thiophen-2-ylmagnesium chloride in THF (0.567 ml, 0.567 mmol). The mixture was stirred at 0°C, then 0.687 ml of the resulting mixture was added to a solution of Ni(dppp)Cl_2 in THF (0.0036 g, 0.010 M). The solution was stirred for 1 hour at 0 °C. The reaction was quenched by adding HCl in THF. The product was analyzed via GC/MS.

*Synthesis of **9a***

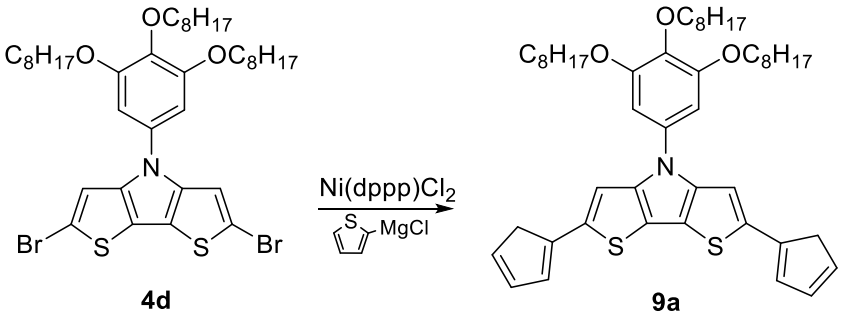

4d (0.457 g, 0.567 mmol) was added to an oven-dried flask, with $Ni(dppp)Cl_2$ (0.0015 g, 0.0028 mmol). The mixture was stirred at 0°C, then a solution of thiophen-2-ylmagnesium chloride in THF (0.567 ml, 0.567 mmol) was added. The solution was stirred for 12 hour at RT. The reaction was quenched with water. The product was analyzed via GC/MS.

5.11 Polymerization via Lewis Acid (General procedure)

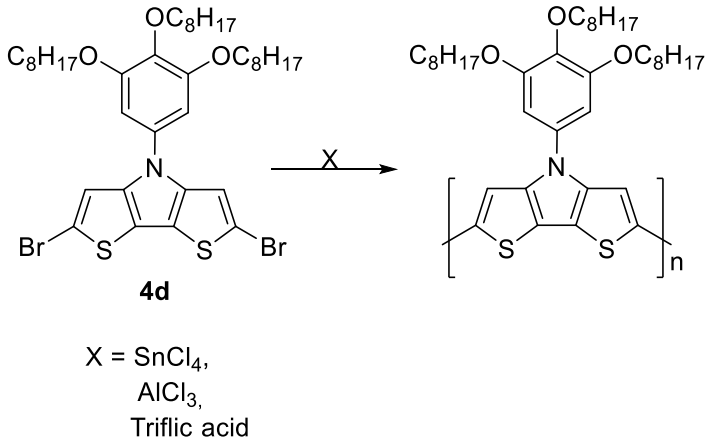

A solution of **4d** (0.33 mmol, 0.263 g) was prepared with 2 ml of anhydrous solvent and stirred. Then, an amount of different Lewis acid was dissolved in 5 ml of anhydrous solvent. Part of this solution was added to the monomer in order to start the polymerization. Solvent, time and temperature of reaction were screened and reported in Table 3.2.1. The product was analyzed by GPC, after quenching the reaction with MeOH and N_2H_4.

4.12 Study of Polymerization (General procedure)

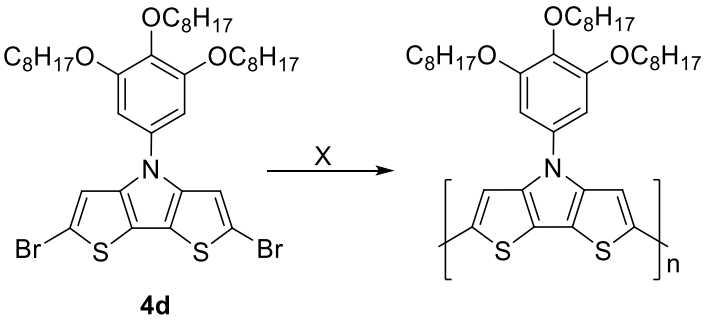

4d

X = $SnCl_4$
Triflic Acid

A solution of **4d** (0.730 mmol, 0.581 g) in 7 ml of anhydrous o-DCB was prepared and stirred. Then, 0.2 ml of this solution was quenched with 10 ml of water and 2-3 drops of N_2H_4. The Lewis acid was then added. The mixture was stirred at 120 °C. At several defined moments, a sample of the polymerization was quenched with water and some drops of N_2H_4, in order to monitored the reaction. The sample was analyzed by GPC.

5.13 Synthesis of sodium 4-(tert-butyl)phenolate (10a)

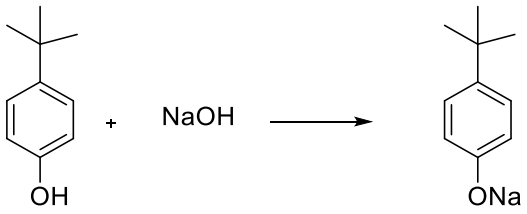

10a

4-(*tert*-butyl)phenol (0.750 g, 0.500 mmole) was dissolved in 2.60 ml of methanol and sodium hydroxide (0.200 g, 0.500 mmol) dissolved in of water (0.40 ml) was added. The solvents were removed by rotary evaporation and by heating the sample at 70 °C for 1 hour under reduced pressure. Once cooled, the crude salt was dissolved in 1.20 ml of THF and the solution was filtered. The filtrate was washed thoroughly with ethyl ether and dried. A white solid was obtained (89 %).

^{1}H-NMR (d6-DMSO, 300Hz, ppm): 6.82 (d, J = 3.0 Hz, 2H); 6.17 (d, J = 3.0 Hz, 2H); 1.20 (s, 9H).

5.14 Synthesis of Sodium 4-(trimethylsilyl)phenolate (11b)

Step 1: Synthesis of 4-(trimethylsilyl)phenol **(11a)**

11a

4- bromophenol (1.73 g, 10.0 mmol) was dissolved in 20 ml of THF and cooled to –78 °C. After that, 9.0 ml of *n*-butyllithium (22.5 mmol, 2.5 M) was added dropwise and the reaction was stirred 1 hour at -78 °C. Then, trimethylsilyl chloride (3.3 mL, 26 mmol) was added and, after 30 minutes, the flask was warmed up to room temperature overnight. The reaction was quenched with HCl (1M); then, the mixture is diluted with water and extracted with EtOAc. The organic layer was washed with $NaHCO_3$ and a saturated solution of NaCl. Once dried with $MgSO_4$, the solvent was removed via rotary evaporation. The crude compound was purified by column chromatography (SiO_2, heptane/DCM, 80/20) to obtain a white solid (0.800 g, 4.81 mmol) with yield of 48 %.

^{1}H-NMR ($CDCl_3$, 300MHz, ppm): δ 6.84 (d, *J* = 3.0 Hz, 2H); 6.04 (d, *J* = 3.0 Hz, 2H); 0.27 (s, 9H).

Step 2: Synthesis of Sodium 4-(trimethylsilyl)phenolate **(11b)**

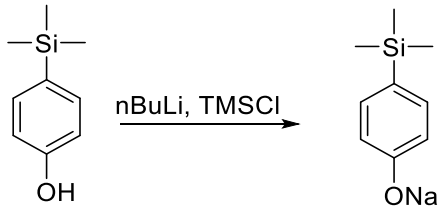

11a **11b**

11a (5.00 mmol, 0.750 g) was dissolved in 2.5 ml of MeOH. NaOH (5.00 mmol, 0.200 g) was dissolved in 0.4 ml of water and was added to the solution. The solvents were removed by rotary evaporation. The solid was dissolved in THF (20 ml) and filtered. The filtrate was added to toluene at 0°C, and a white solid was formed (72 %). The solid was filtered and analyzed via ^{1}H NMR.

^{1}H-NMR (d6-DMSO, 300MHz, ppm): δ 6.84 (d, *J* = 3.0 Hz, 2H); 6.05 (d, *J* = 3.0 Hz, 2H); 0.08 (s, 9H).

5.15 Polymerization with endcapping (General procedure)

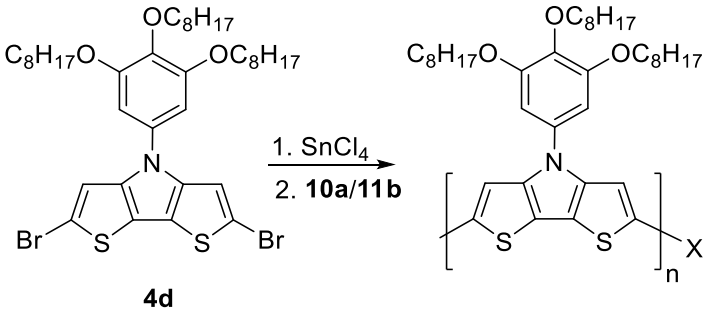

4d

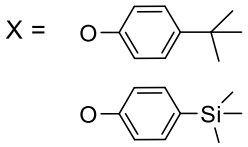

To a solution of **4d** (0.100 g, 0.333 mmol) in 2.0 ml of anhydrous o-DCB at 120 ºC, was added 0.200 ml of a solution of $SnCl_4$ (5%, $1.65 \cdot 10^{-2}$ mmol) in anhydrous o-DCB. The resulting mixture was stirred at 120 ºC for 24 hours, then it was transferred to a suspension of 0.5 mmol of the end capper in o-DCB (1 ml) by cannula. The mixture was stirred overnight, then was poured into MeOH (200 ml) and few drops (4-10) of hydrazine hydrate were added. The solution was stirred for 1 h to allow the precipitation of the product; the resulting solid was filtered and washed with MeOH (200 ml) and filtered into a Soxhlet thimble. Soxhlet extractions were performed with different solvents in order to remove impurities and oligomers. A subsequent Soxhlet extraction with chloroform was used to extract the polymer. After removing the solvent, a purple solid was obtained. The product was analyzed by GPC.

5.16 “Sergeants and solders” experiment (General procedure)

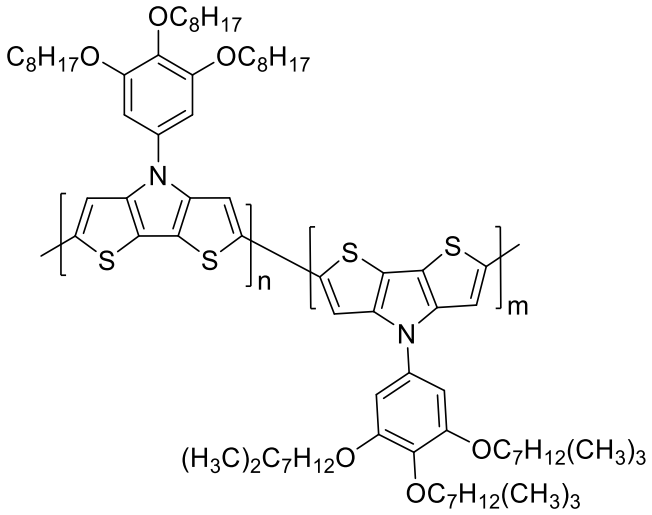

Different amount of **5d** and **4d** were prepared in 2 ml of dried o-DCB. 0.2 ml of a solution of $SnCl_4$ (5%, $1.65 \cdot 10^{-2}$ mmol) was added to the flask. The reaction was stirred at RT for 48 hours at 120 °C and quenched adding a solution of MeOH with 4-10 drops of hydrazine. Soxhlet extractions with acetone was performed in order to remove impurities and oligomers. A subsequent Soxhlet extraction with chloroform was used to extract the polymer. After removing the solvent a purple solid was obtained. Every samples were analyzed by CD, GPC and ^{1}H NMR.

5.17 Block copolymerization with butyl vinyl ether

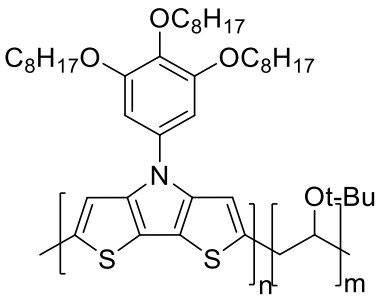

To a solution of **4d** (0.100 g, 0.333 mmol) in 3.0 ml of anhydrous toluene at 120 ºC, 0.2 ml of a solution of $SnCl_4$ (5%, $1.65 \cdot 10^{-2}$ mmol) in anhydrous o-DCB was added. After 72 hours, 2

mmol of butyl vinyl ether in 5 ml of dry toluene at -78 °C was added. The reaction was stirred at RT for 24 hours and quenched adding a solution of MeOH with 4-10 drops of hydrazine. Soxhlet extractions were performed with acetone in order to remove impurities and oligomers. A subsequent Soxhlet extraction with chloroform was used to extract the polymer, and after removing the solvent a purple solid was obtained. The product was analyzed by GPC and ^{1}H NMR.

5.18 Synthesis of 2-chloro-3-(octyloxy)thiophene (12b)

Step 1: Synthesis of 3-(octyloxy)thiophene **(12a)**

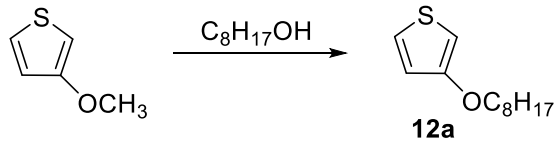

12a

To a solution of 3-methoxythiophene (3.53 g, 30.9 mmol), octan-1-ol (8.06 g, 61.9 mmol) and *para*-toluenesulfonic acid in toluene (1.24 mmol, 0.148 g) in 30 mL were added. The solution was refluxed and stirred for 3 days. After cooling down, 50 ml of water was added and the organic layer was extracted, washed with Na_2CO_3 (2x20 mL) and dried with anhydrous magnesium sulfate. The solvent was removed under reduced pressure and the resulting material was purified by column chromatography (SiO_2, heptane/DCM, 90/10), obtaining a yellow viscous oil with yield of 76 %.

^{1}H-NMR ($CDCl_3$, 300Hz, ppm): δ 7.17 (dd, J = 5.3, 3.1 Hz, 1H); 6.75 (dd, J = 5.2, 1.5 Hz, 1H); 6.22 (dd, J = 3.1, 1.5 Hz, 1H); 3.93 (2H, t); 1.8 – 0.8 (15H, m).

Step 2: Synthesis of 2-chloro-3-(octyloxy)thiophene **(12b)**

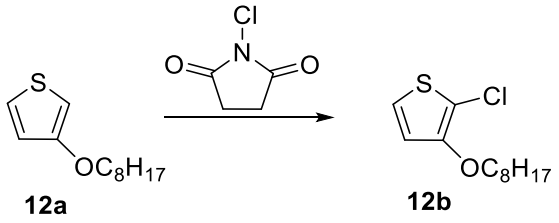

12a **12b**

A solution of **12a** (2.28 g, 10.8 mmol) in DMF (20 mL) was stirred at 0 ºC, and *N*-chlorosuccinimide (1.37 g,10.2 mmol) in 5 mL of DMF was added dropwise. The reaction mixture was warmed until room temperature and stirred overnight. 20 ml of water was added and the reaction mixture was washed with ethyl acetate. The organic fraction was dried with $MgSO_4$ and the solvent was removed via rotary evaporation. The resulting material was purified by column chromatography (SiO_2, heptane/EtOAc, 90/10), obtaining a colorless oil (yield 54 %).

^{1}H-NMR ($CDCl_3$, 300MHz, ppm): δ 6.99 (d, *J* = 6.0 Hz, 1H); 6.76 (d, *J* = 6.0 Hz, 1H); 4.03 (2H, t); 1.74 – 0.8 (15H, m).

5.19 Block copolymerization with 12b (General procedure)

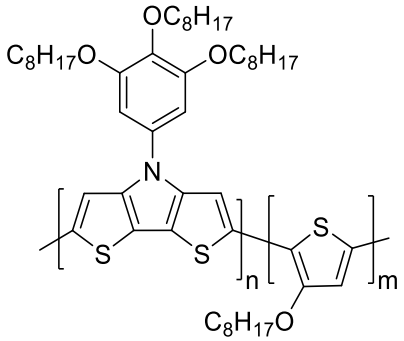

To a solution of (the first) monomer (0.333 mmol) in 2.0 ml of anhydrous o-DCB at 120 ºC, was added 0.2 ml of a solution of $SnCl_4$ (10%, $3.33 \cdot 10^{-2}$ mmol) in anhydrous o-DCB. After

48 hours, a solution of (the second) monomer (0.33 mmol in 1.5 ml of o-DCB) was added. The reaction was stirred for 48 hours. A Soxhlet extraction was performed with acetone in order to remove impurities and oligomers. A subsequent Soxhlet extraction with chloroform was used to extract the polymer. The solvent was removed under vacuum and solid was obtained. The product was analyzed by GPC.

ACKNOWLEDGES

Firstly, I would like to express my sincere gratitude to Professor Guy Koeckelberghs for hosting me and for his enthusiasm and encouragement. I greatly appreciate also the help and the moments together with all the colleagues of LPS group.

I would like to thank Professor Elisabetta Salatelli, who provided me the opportunity to join this research group. Moreover, I thank her for the helping me during the writing of this thesis.

Thanks to my mentor, Pieter Leysen, for his patience, motivation and knowledge. I really treasured everything he taught me.

Thanks to Tomas, who went through this with me, and to my beloved “Red Carpet friends” to have been my family during my Erasmus.

Finally, to my family and Italian friends, thanks for everything: this is as much yours as mine.